Highly Reflective Foveal Region in Optical Coherence Tomography in Eyes with Vitreomacular Traction or Epiretinal Membrane

Kazushige Tsunoda, MD,[1] Ken Watanabe, MD,[2] Kunihiko Akiyama, MD,[2] Tomoaki Usui, MD,[3] Toru Noda, MD[2]

Objective: To report the optical coherence tomography (OCT) findings in eyes with vitreomacular traction (VMT) or with an epiretinal membrane (ERM).

Design: Retrospective case series.

Participants: Fifty-four eyes of 45 consecutive patients with subjective visual disturbances resulting from VMT or idiopathic ERM were studied.

Methods: The morphologic features of the photoreceptor layer at the foveal center were determined and the central foveal thickness (CFT) was measured by spectral-domain (SD) OCT.

Main Outcome Measures: The morphologic characteristics of the foveal region observed by SD OCT.

Results: A roundish or diffuse highly reflective region was observed between the photoreceptor inner segment/outer segment junction line and the cone outer segment tip line at the center of the fovea. This highly reflective region was present in 7 of 7 cases of VMT and 30 of 47 cases of ERM. In the ERM cases, the mean CFT of the cases with the highly reflective region was significantly thicker than that in cases without it. The highly reflective region disappeared when the inward traction on the fovea was released surgically or spontaneously.

Conclusions: The highly reflective region is a characteristic sign observed in the OCT images of eyes with VMT and ERM, and it has been termed the *cotton ball sign* after its appearance. The presence of the cotton ball sign indicates an inward traction on the fovea and may be a predictor of visual impairment.

Financial Disclosure(s): The author(s) have no proprietary or commercial interest in any materials discussed in this article. *Ophthalmology 2012;119:581–587*

Vitreomacular tractions (VMTs) and epiretinal membranes (ERMs) cause morphologic distortions of the retinal surface and lead to functional changes such as metamorphopsia and decreased visual acuity.[1–4] Surgical removal of the VMT or ERM is effective in restoring good visual function. Similar recovery is obtained when the traction is released spontaneously.

Optical coherence tomography (OCT) has shown that a vertical or tangential traction of the retina causes wrinkling of the internal limiting membrane, flattening of the foveal pit, and intraretinal cystic changes.[5–11] Moreover, recent spectral-domain (SD) OCT has shown that eyes with VMT and ERM have structural abnormalities of the photoreceptors at the fovea, for example, loss of the photoreceptor inner/outer segment (IS/OS) junction line.[12–17] The abnormalities in the IS/OS junction line were correlated significantly with poorer visual function; however, the relationship between these abnormal OCT findings and the foveal traction has not been determined definitively. The SD OCT studies have shown a roundish or diffuse highly reflective region at the center of the fovea in all of the cases of VMT and in cases of ERM with increased central foveal thickness (CFT). The authors named this highly reflective region the *cotton ball sign*, after its appearance.

The aim of this study was to determine the characteristics and correlations of this abnormal sign in the OCT images and the retinal physiologic features. This study showed that the cotton ball sign disappeared when the foveal traction was released surgically or spontaneously. The presence of the cotton ball sign is good evidence that there is inward traction on the photoreceptors.

Patients and Methods

This was a retrospective case series performed in the Department of Ophthalmology, National Tokyo Medical Center, Tokyo, Japan. Informed consent was obtained from all of the subjects for the tests after an explanation of the procedures to be used. The procedures used adhered to the tenets of the Declaration of Helsinki, and approval to perform this study was obtained from the Review Board/Ethics Committee of the National Tokyo Medical Center.

ISSN 0161-6420/12/$–see front matter
doi:10.1016/j.ophtha.2011.08.026

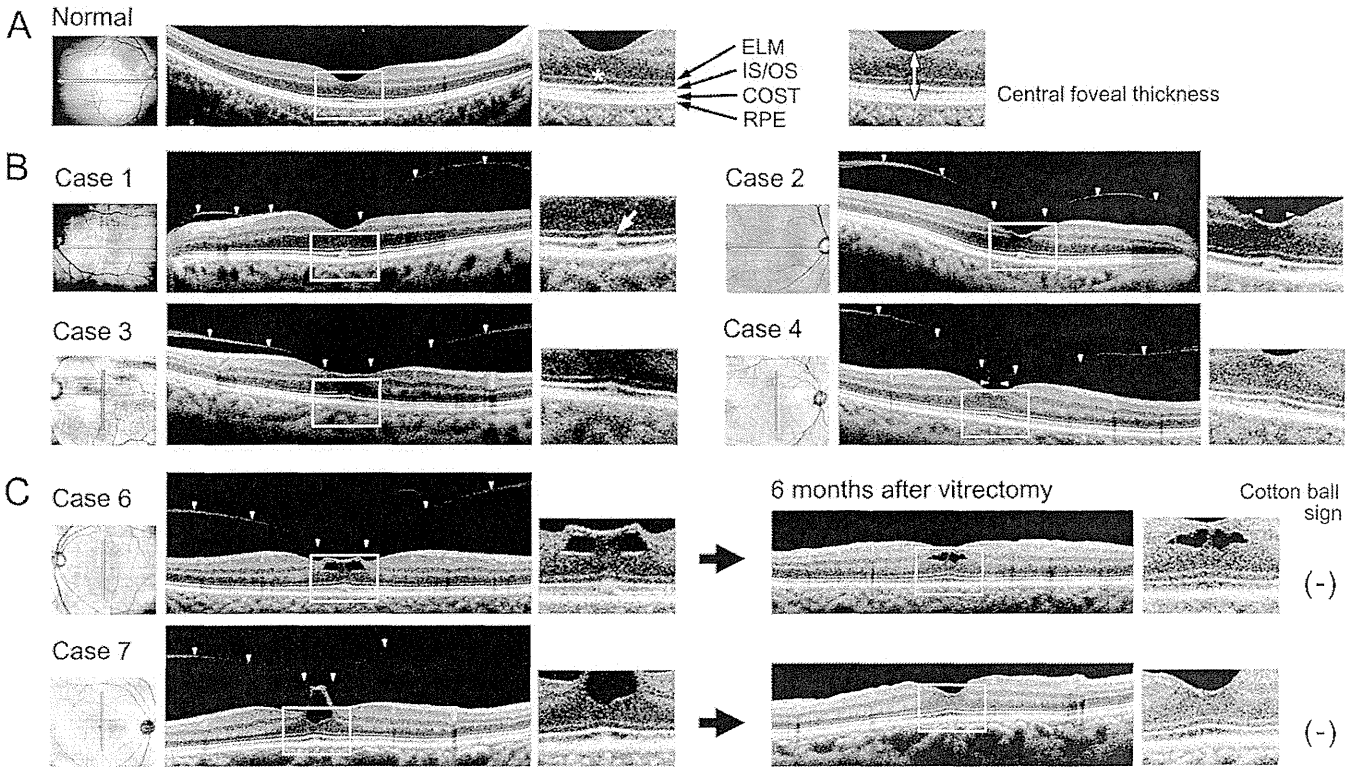

Figure 1. Optical coherence tomography (OCT) images of eyes with vitreomacular traction (VMT) with the foveal images magnified on the right. Fundus images on the left indicate the location of the OCT scans. **A**, Normal control OCT image from a 22-year-old woman. Outer retinal structures with high reflectivity are indicated by arrows: external limiting membrane (ELM), photoreceptor inner segment/outer segment (IS/OS) junction, cone outer segment tip (COST) line, and retinal pigment epithelium (RPE). The foveal bulge is indicated by an *asterisk*. The central foveal thickness is measured as the distance between the inner retinal surface and inner border of the RPE (*white arrow*). **B**, Optical coherence tomography images of eyes with VMT. The border of the posterior vitreous is indicated by *arrowheads*. The roundish highly reflective region between IS/OS junction line and COST line is the cotton ball sign and is identified by a *white arrow* in case 1. **C**, Two eyes with VMT before and 6 months after vitrectomy. In both cases, the vitreous traction was released and the cotton ball sign was not present after the surgery.

Inclusion and Exclusion Criteria

Fifty-four eyes of 45 patients (average age, 69.0±9.2 years; range, 34–85 years) with subjective visual disturbances resulting from VMT or idiopathic ERM were studied. The patients were examined between October 2009 and January 2011; 7 eyes had VMT and 47 eyes had ERM (Table 1, available at http://aaojournal.org). A VMT was defined as a vitreomacular adhesion at the foveal region without an apparent ERM over the entire macular region. All of the cases with VMT were focal VMT, according to the definition of Koizumi et al.[11] The exclusion criteria were: (1) eyes with a history of retinal inflammatory or vascular diseases, such as branch vein occlusion, uveitis, and retinal detachment; (2) eyes with advanced lens opacification or any other ocular diseases that could cause visual disturbances; (3) eyes with strong vitreal traction on the retina that led to either lamellar or pseudomacular holes; (4) eyes in which the center of the fovea could not be determined in the OCT images because of a lack of a bulge-like structure of the IS/OS junction line at the fovea[18]; and (5) cases whose OCT image did not have enough signal intensity for evaluation, that is, average intensity of the OCT signal less than 8/10.

All patients underwent a complete ophthalmologic examination, including best-corrected visual acuity using a Landolt C chart, biomicroscopy of the fundus, fundus photography, and OCT.

Optical Coherence Tomography

The OCT images were obtained with SD OCT (Cirrus HD-OCT, versions 4.5 and 5.1; Carl Zeiss Meditec, Dublin, CA). After dilatation of the pupil, patients were asked to fixate on a target, and 5-line scans with 4 averages were performed both horizontally (length, 9.0 mm) and vertically (length, 6.0 mm). The distance between each scan line was set to be 0.075 mm, or, in some cases, 0.025 mm, to determine the location of foveal bulge. The foveal bulge is a dome-shaped structure of the IS/OS junction line corresponding to the foveal center (Fig 1A, asterisk). If the foveal bulge could not be obtained by the point of fixation, the location of the scan line was shifted and the OCT images were taken repeatedly until the foveal bulge was present in the image.

The CFT was defined as the distance between inner retinal surface and inner border of retinal pigment epithelium (RPE; Fig 1A) and was measured with the built-in scale of the OCT system. The diameter of the highly reflective region was measured in one of the scanned profiles that showed the maximum diameter of the region. For patients who underwent vitrectomy, the OCT images were recorded 6 months after the surgery.

Vitrectomy for Vitreomacular Traction and Epiretinal Membranes

Two of 7 eyes with VMT and 18 of 47 eyes with an ERM underwent 23- or 25-gauge 3-port vitrectomy by 2 experienced

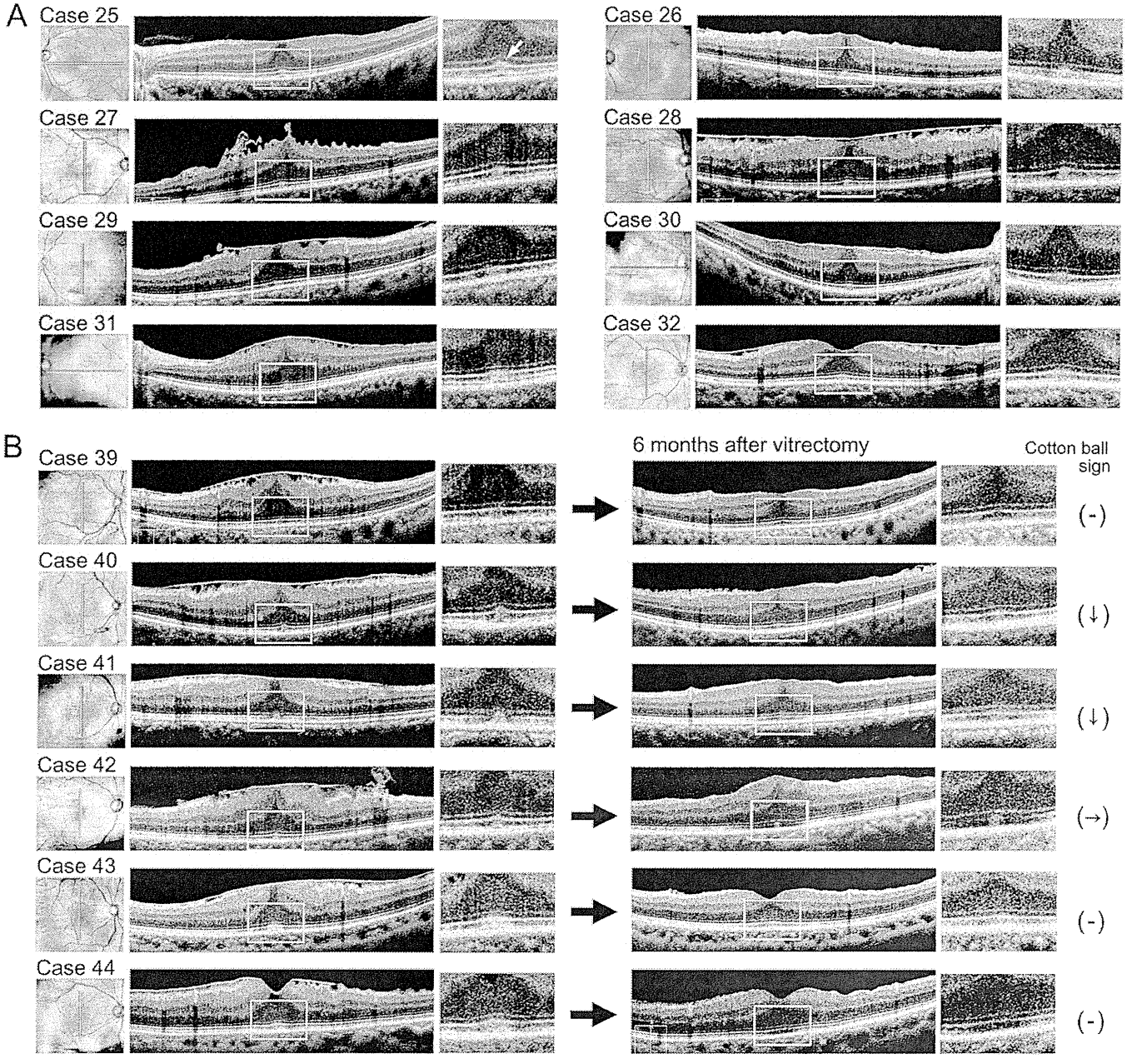

Figure 2. Optical coherence tomography (OCT) images of eyes with an epiretinal membrane (ERM) with the foveal area magnified (*right*). Fundus photographs (*left*) indicate the location of OCT scans. **A**, Optical coherence tomography images of eyes with an ERM. The roundish highly reflective region between inner segment/outer segment junction line and cone outer segment tip line is the cotton ball sign and is identified by a *white arrow* in case 25. **B**, Optical coherence tomography images of eyes with an ERM before and 6 months after vitrectomy. In cases 39, 43, and 44, the cotton ball sign disappeared after surgery. In cases 40 and 41, the cotton ball sign did not disappear, but became more indistinct after the surgery. In case 42, the cotton ball sign was still observed clearly after the surgery. The highly reflective region in cases 25, 40, and 41 appeared roundish, but that in cases 31, 43, and 44 appeared indistinct and diffuse.

surgeons (K.A. and K.W.). During the vitrectomy, a posterior hyaloid detachment was made, and the ERM was removed. The internal limiting membrane was peeled with forceps in all cases. Phacoemulsification with intraocular lens implantation was performed during the same surgery in 17 of the 20 eyes.

Statistical Analysis

Student *t* tests were performed to compare the CFT with the presence of the highly reflective region in cases of ERM before and after surgery. Statistical analysis was performed using Microsoft Office Excel 2007 (Microsoft, Redmond, WA). *P* values <0.05 were taken as statistically significant.

Results

The outer retinal structures detected in the OCT image of normal retinas consisted of (1) the external limiting membrane, (2) the IS/OS junction line, (3) the cone outer segment tip (COST) line,

Table 2. Cotton Ball Sign and Central Foveal Thickness

	Cotton Ball Sign	Central Foveal Thickness (μm)		P
		Mean	*Standard Deviation*	
VMT (n = 7)	Observed	252.0	87.1	
ERM before surgery (n = 47)	Not observed (n = 17)	289.3	96.0	0.0000076*
	Observed (n = 30)	445.7	102.2	
	Total (n = 47)	389.1	124.7	
ERM after surgery (n = 16)	Disappeared (n = 8)	300.0	28.6	0.00033†
	Not disappeared (n = 8)	423.3	59.0	

ERM = epiretinal membrane; VMT= vitreomacular traction.
*t test between ERM with and without cotton ball sign.
†t test between ERM with and without the disappearance of cotton ball sign after vitrectomy.

(4) the RPE, and (5) the foveal bulge, which is a dome-like structure of the external limiting membrane and IS/OS junction line caused by an elongation of the cone outer segments at the fovea (Fig 1A).[18–20]

A highly reflective region was present in all of the eyes with VMT (Table 1, available at http://aaojournal.org). The OCT images of 6 VMT cases without (Fig 1B) or with (Fig 1C) vitrectomy are shown with the foveal images magnified. In all the cases, a separation of the vitreous from the retina occurred except in the limited region around the center of the fovea (Fig 1A, B, arrowheads), and the foveal center was pulled toward the vitreous cavity. In case 1, a roundish, highly reflective region resembling a cotton ball can be seen between the IS/OS junction line and COST line at the center of the fovea. The COST line can be seen to be pulled inward just below the highly reflective region and is separated from the RPE (Fig 1B, case 1, white arrow). Similar findings were observed in cases 2 and 6. In all of the other cases (cases 3, 4, and 7), the highly reflective region was observed at the same location, but its borders were more indistinct than in cases 1, 2, and 6. Two of the eyes with VMT underwent vitrectomy, and the highly reflective region could not be observed in the OCT image obtained 6 months after the vitrectomy (Table 1, available at http://aaojournal.org; Fig. 1C).

The SD OCT examinations of the 47 eyes with an ERM showed that the highly reflective region was present in 30 eyes (63.8%; Table 1, available at http://aaojournal.org). The OCT images of 8 ERM cases without (Fig 2A) or with (Fig 2B) treatment are shown with the foveal images magnified. In all the cases, the epiretinal membrane covered the entire macular region, and the tangential traction elevated the retinal surface at the fovea, leading to a loss of the foveal pit. In case 25, the highly reflective region was observed between the IS/OS junction line and COST line at the center of the fovea (Fig 2A, case 25, white arrow). As in the eyes with VMT, the COST line was pulled inward just below the highly reflective region and was separated from the RPE. The highly reflective region was observed at the same location in all eyes. The regions appeared roundish in some cases (e.g., cases 25, 40, and 41) and indistinct and diffuse in other cases (e.g., cases 31, 43, and 44).

Vitrectomy was performed on 16 eyes with an ERM, and 6 months after surgery, the highly reflective region was not observed in 8 cases, became smaller and more indistinct in 2 cases, or could still be observed in 6 cases (Table 1, available at http://aaojournal.org; Fig 2B).

The diameter of the highly reflective region varied from 96 to 180 μm with a mean 130.4±36.4 μm in the eyes with a VMT and from 80 to 288 μm with a mean of 172.7±65.8 μm in eyes with an ERM. The highly reflective region was always present between the IS/OS junction and COST lines, except for case 41, where the IS/OS junction line was disrupted at the foveal center and the round, highly reflective region penetrated into the outer nuclear layer (Fig 2B).

The mean CFT was 252.0±87.1 μm in eyes with VMT and 389.1±124.7 μm in eyes with an ERM (Table 2). For the 47 eyes with an ERM, the mean CFT of the eyes with the highly reflective region was 445.7±102.2 μm, which was significantly thicker than that in eyes without the highly reflective region at 289±96.0 μm. For the 16 eyes with an ERM for which vitrectomy was performed, the CFT was measured 6 months after surgery. The mean CFT of the 8 eyes in which the highly reflective region did not disappear was 423.3±59.0 μm, which was significantly thicker than that in the 8 eyes in which the highly reflective region disappeared at 300.0±28.6 μm.

In one case (case 5) with a spontaneous vitreous detachment, there was a recovery of the microstructural damage of the photoreceptor layer in the OCT images. Case 5 was a 34-year-old woman who had a sudden decrease of her vision together with floaters in her right eye (Table 1, available at http://aaojournal.org; Fig 3). Her best-corrected visual acuity was 0.6 in the right eye and 1.2 in the left eye. She was referred to the authors' hospital 10 days after the onset of her symptoms, and fundus biomicroscopic examination showed that a thick posterior hyaloid membrane was detached from the posterior pole in her right eye. In the OCT image, there was a clear, highly reflective region, although the vitreomacular traction had been released (Fig 3A). Moreover, the photoreceptor IS/OS junction line seemed to be pulled inward at the foveal center, and there was a local defect of the COST line just beneath the highly reflective region (Fig 3A, white arrow). In the OCT image obtained 30 days after the onset, the highly reflective region was not present, and the photoreceptor structures, including the IS/OS junction and COST lines, appeared normal (Fig 3B, white arrow). The visual acuity also recovered to 1.0 at that time.

Discussion

The SD OCT findings showed that all eyes (n = 7) with VMT and 63.8% of the eyes (30/47) with an ERM have a highly reflective region at the center of the fovea. This region can be roundish in some cases or diffuse and indistinct in other cases, and it was always located between the IS/OS junction and COST lines. This area was termed the *cotton ball sign* after its appearance. Related articles were searched for in PubMed with the following terms: *vitreomacular traction*, *epiretinal membrane*, and *optical coher-*

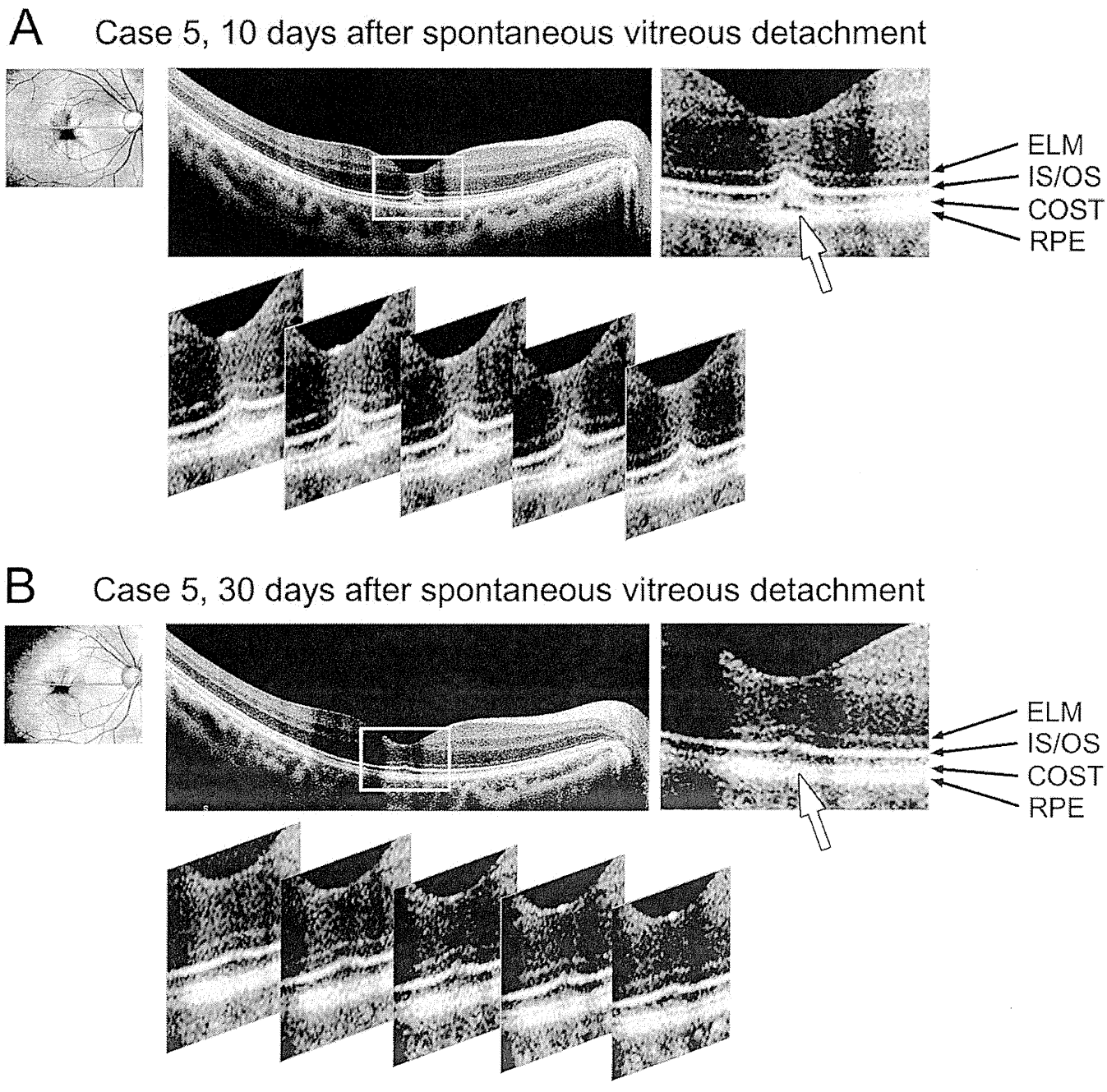

Figure 3. Optical coherence tomography (OCT) images of eyes with vitreomacular traction (case 5) in which a posterior vitreous detachment occurred spontaneously without surgery. Five horizontal OCT scans were obtained with an interscan distance of 20 μm. Five sequential profiles of the foveal region are aligned at the bottom, covering the central region of 80 μm of the fovea. **A**, Optical coherence tomography image obtained 10 days after spontaneous vitreous detachment. A round, highly reflective region (cotton ball sign) is present between the inner segment/outer segment (IS/OS) junction and cone outer segment tip (COST) lines at the foveal center. The center of IS/OS junction line is pulled inward and appears protruded compared with that in a normal OCT image (Fig 1A). The COST line is disrupted just below the highly reflective region (*white arrow*). **B**, Optical coherence tomography image obtained 30 days after the spontaneous vitreous detachment. The cotton ball sign is not present. The protrusion of IS/OS junction line is not distinct, and the COST line is continuous over the entire foveal region (*white arrow*). ELM = external limiting membrane; RPE = retinal pigment epithelium.

ence tomography. These articles were read, and none of them describes the same feature.

Even with the improved OCT instruments with higher spatial resolution, the region easily can be missed if the scanned lines do not pass through the foveal center, the intensity of the OCT signal is not strong enough, or both. Three-dimensional volume scans do not have enough traverse resolution, so OCT should be made with multiple scans with the highest resolution available. The mean diameter of the highly reflective region varied from 96 to 180 μm with a mean of 130.4±36.4 μm in the eyes with VMT and from 80 to 288 μm with a mean of 172.7±65.8 μm in

eyes with an ERM. This means that the distance between each scan line should be set to less than 75 μm in the Cirrus HD-OCT. For example, the consecutive OCT images of case 5 were obtained with 5-line scans with a distance between the scans of 20 μm (Fig 3A, bottom). Moreover, because the fixation point is sometimes shifted upward in cases of longstanding ERM, the OCT scan should be repeated until the true center of the fovea is scanned.

The cotton ball sign in the OCT images seemed to be strongly correlated with the inward traction on the retina. In eyes with VMT, local adhesions between the vitreous and retinal surface causes strong and direct inward traction over the entire depth of the foveal pit.[13,16] However, an ERM causes a tangential shrinkage of the retinal surface, and this leads to an inward retinal displacement of the fovea, regardless of the existence of a posterior vitreous detachment. This continuous tension also affects the photoreceptor layer, leading to mechanical damage of the photoreceptors and deterioration of visual function.[12,14,15] In this study, in eyes with VMT in which direct vitreous traction was present at the fovea, the cotton ball sign was always observed, although there was no apparent inward displacement of the fovea in cases 1 through 5 (Figs 1 and 3) and the CFT was normal, except in cases 6 and 7 (Table 1, available at http://aaojournal.org). In the eyes with an ERM, the mean CFT of the cases with the cotton ball sign was significantly thicker than that in eyes without the cotton ball sign (Table 2). These findings indicate that the continuous inward traction by the ERM was the cause of the cotton ball sign. In 8 of 16 cases that underwent vitrectomy, the cotton ball sign disappeared within 6 months and the CFT was significantly thinner than that in eyes where the cotton ball sign did not disappear. This indicated that disappearance of the highly reflective region was not the result of the removal of the ERM, but was most likely the result of the release of inward traction. It is notable that in cases where the cotton ball sign disappeared after surgery, the foveal pit reappeared because of release of inward traction (Fig 2B, cases 39, 43, and 44). However, in cases where the cotton ball sign did not disappear, the foveal area was still flat or even convex (Fig 2B, cases 40, 41, and 42). These highly reflective regions were observed only at the foveal center, even in cases where the entire macular region was thickened because of the ERM. There are 2 possible reasons for why the cotton ball sign is observed only at the foveal center in the ERM eyes. First, in cases in which the internal limiting membrane became flat because of the tangential traction by the ERM, the inward traction could be applied most strongly to the photoreceptors at the foveal center because of the presence of the foveal pit. Second, the cone photoreceptors at the fovea have an elongated shape and their diameter is much smaller than those at the parafoveal region. This characteristic anatomic structure makes them more susceptible to the minute structural changes that may lead to the increased reflectivity in the OCT.

An ERM usually is associated with macular edema and reduced reflectivity resulting from fluid accumulation; however, an increase in the reflectivity is observed rarely. Then the question arises on why the inward traction affected the reflectivity of the foveal center in the OCT images? The highly reflective region was always located between the IS/OS junction and COST lines. This region corresponds to the outer segment of cone photoreceptors, whose reflectivity is usually low. The photoreceptor outer segments (OSs) contain stacks of membranous discs that are rich in visual pigments, and the OSs are aligned parallel to the light pathway. The authors suggest that the inward traction on the retina changes the alignment of the OSs, which then increases their reflectivity. Directional reflectivity is known to exist in the retinal nerve fiber layer[21,22] and Henle's fiber layer.[23] Recently, Lujan et al[23] successfully distinguished Henle's fiber layer from the true outer nuclear layer by varying the angular incidence of the OCT beam on the retinal plane. The photoreceptor OSs are long cylindrical structures whose reflectivity may depend on the angular incidence of the OCT beam.

The second hypothesis for the highly reflective region is that the continuous inward traction causes microstructural damages to the cone OSs, leading to glial migration, glial scar formation, and photoreceptor degeneration.[24] However, it is not likely that these changes could be reversible and, particularly in case 5, would completely recover within 30 days after the release of mechanical traction (Fig 3, case 5).

The exact mechanism causing the highly reflective region was not determined, but there is very little possibility that this highly reflectivity region is an optical artifact, because it appeared when inward traction was forced to the outer retina, regardless of the existence of an ERM, and disappeared when the traction was released.

The cotton ball sign was present, despite good vision in the patients; 4 of 7 eyes with VMT and 9 of 30 eyes with an ERM with the cotton ball sign had best-corrected visual acuity of 0.8 or better (Table 1, available at http://aaojournal.org). This means that the cotton ball sign does not necessarily indicate a decrease in visual acuity, and it may be used as a predictor of visual impairment that would arise after longstanding inward traction at the fovea. Continuous foveal traction is known to cause microstructural damages in the photoreceptor layer,[12–16] and early detection of this sign may help in the management of these patients in preserving good vision.

References

1. Jaffe NS. Vitreous traction at the posterior pole of the fundus due to alterations in the vitreous posterior. Trans Am Acad Ophthalmol Otolaryngol 1967;71:642–52.
2. Wise GN. Relationship of idiopathic preretinal macular fibrosis to posterior vitreous detachment. Am J Ophthalmol 1975; 79:358–62.
3. Smiddy WE, Maguire AM, Green WR, et al. Idiopathic epiretinal membranes: ultrastructural characteristics and clinicopathologic correlation. Ophthalmology 1989;96:811–20; discussion 821.
4. Gandorfer A, Rohleder M, Kampik A. Epiretinal pathology of vitreomacular traction syndrome. Br J Ophthalmol 2002;86: 902–9.
5. Puliafito CA, Hee MR, Lin CP, et al. Imaging of macular diseases with optical coherence tomography. Ophthalmology 1995;102:217–29.

6. Wilkins JR, Puliafito CA, Hee MR, et al. Characterization of epiretinal membranes using optical coherence tomography. Ophthalmology 1996;103:2142–51.
7. Meyer CH, Rodrigues EB, Mennel S, et al. Spontaneous separation of epiretinal membrane in young subjects: personal observations and review of the literature. Graefes Arch Clin Exp Ophthalmol 2004;242:977–85.
8. Johnson MW. Tractional cystoid macular edema: a subtle variant of the vitreomacular traction syndrome. Am J Ophthalmol 2005;140:184–92.
9. Schmidt-Erfurth U, Leitgeb RA, Michels S, et al. Three-dimensional ultrahigh-resolution optical coherence tomography of macular diseases. Invest Ophthalmol Vis Sci 2005;46:3393–402.
10. Legarreta JE, Gregori G, Knighton RW, et al. Three-dimensional spectral-domain optical coherence tomography images of the retina in the presence of epiretinal membranes. Am J Ophthalmol 2008;145:1023–30.
11. Koizumi H, Spaide RF, Fisher YL, et al. Three-dimensional evaluation of vitreomacular traction and epiretinal membrane using spectral-domain optical coherence tomography. Am J Ophthalmol 2008;145:509–17.
12. Michalewski J, Michalewska Z, Cisiecki S, Nawrocki J. Morphologically functional correlations of macular pathology connected with epiretinal membrane formation in spectral optical coherence tomography (SOCT). Graefes Arch Clin Exp Ophthalmol 2007;245:1623–31.
13. Gaudric A. Macular cysts, holes and cavitations: 2006 Jules Gonin lecture of the Retina Research Foundation. Graefes Arch Clin Exp Ophthalmol 2008;246:1071–9.
14. Suh MH, Seo JM, Park KH, Yu HG. Associations between macular findings by optical coherence tomography and visual outcomes after epiretinal membrane removal. Am J Ophthalmol 2009;147:473–80.
15. Falkner-Radler CI, Glittenberg C, Hagen S, et al. Spectral-domain optical coherence tomography for monitoring epiretinal membrane surgery. Ophthalmology 2010;117:798–805.
16. Takahashi A, Nagaoka T, Ishiko S, et al. Foveal anatomic changes in a progressing stage 1 macular hole documented by spectral-domain optical coherence tomography. Ophthalmology 2010;117:806–10.
17. Odrobina D, Michalewska Z, Michalewski J, et al. Long-term evaluation of vitreomacular traction disorder in spectral-domain optical coherence tomography. Retina 2011;31:324–31.
18. Tsunoda K, Fujinami K, Miyake Y. Selective abnormality of cone outer segment tip line in acute zonal occult outer retinopathy as observed by spectral domain optical coherence tomography. Arch Ophthalmol 2011;129:1099–101.
19. Srinivasan VJ, Monson BK, Wojtkowski M, et al. Characterization of outer retinal morphology with high-speed, ultra-high-resolution optical coherence tomography. Invest Ophthalmol Vis Sci 2008;49:1571–9.
20. Fernandez EJ, Hermann B, Povazay B, et al. Ultrahigh resolution optical coherence tomography and pancorrection for cellular imaging of the living human retina. Opt Express [serial online] 2008;16:11083–94. Available at: http://www.opticsinfobase.org/abstract.cfm?URI=oe-16-15-11083. Accessed August 9, 2011.
21. Knighton RW, Huang XR. Directional and spectral reflectance of the rat retinal nerve fiber layer. Invest Ophthalmol Vis Sci 1999;40:639–47.
22. Knighton RW, Qian C. An optical model of the human retinal nerve fiber layer: implications of directional reflectance for variability of clinical measurements. J Glaucoma 2000;9:56–62.
23. Lujan B, Roorda A, Knighton RW, Carroll J. Revealing Henle's fiber layer using spectral domain optical coherence tomography. Invest Ophthalmol Vis Sci 2011;52:1486–92.
24. Schuman SG, Koreishi AF, Farsiu S, et al. Photoreceptor layer thinning over drusen in eyes with age-related macular degeneration imaged in vivo with spectral-domain optical coherence tomography. Ophthalmology 2009;116:488–96.

Footnotes and Financial Disclosures

Originally received: March 17, 2011.
Final revision: June 20, 2011.
Accepted: August 11, 2011.
Available online: November 23, 2011. Manuscript no. 2011-444.

[1] Laboratory of Visual Physiology, National Institute of Sensory Organs, Tokyo, Japan.

[2] Department of Ophthalmology, National Tokyo Medical Center, Tokyo, Japan.

[3] Akiba Eye Clinic, Niigata, Japan.

Financial Disclosure(s):
The author(s) have no proprietary or commercial interest in any materials discussed in this article.

Supported in part by research grants from the Ministry of Health, Labor and Welfare, Tokyo, Japan; and the Japan Science and Technology Agency, Tokyo, Japan.

Correspondence:
Kazushige Tsunoda, Laboratory of Visual Physiology, National Institute of Sensory Organs, 2-5-1 Higashigaoka, Meguro-ku, Tokyo 152-8902, Japan. E-mail: tsunodakazushige@kankakuki.go.jp.

lone for the study. Allergan, Inc has provided unrestricted funds to DRCR.net for its discretionary use.

Role of the Sponsor: The funding organization participated in oversight of the conduct of the study and review of the manuscript but not directly in the design of the study, the conduct of the study, data collection, data management, data analysis, interpretation of the data, or preparation of the manuscript. As per the DRCR.net Industry Collaboration Guidelines (http://www.drcr.net), DRCR.net had complete control over the design of the protocol, ownership of the data, and all editorial content of presentations and publications related to the protocol.

1. Diabetic Retinopathy Clinical Research Network. A randomized trial comparing intravitreal triamcinolone acetonide and focal/grid photocoagulation for diabetic macular edema. *Ophthalmology*. 2008;115(9):1447-1449, 1449, e1-e10.
2. Bakri SJ, Pulido JS, McCannel CA, Hodge DO, Diehl N, Hillemeier J. Immediate intraocular pressure changes following intravitreal injections of triamcinolone, pegaptanib, and bevacizumab. *Eye (Lond)*. 2009;23(1):181-185.
3. Benz MS, Albini TA, Holz ER, et al. Short-term course of intraocular pressure after intravitreal injection of triamcinolone acetonide. *Ophthalmology*. 2006; 113(7):1174-1178.
4. Jonas JB, Degenring RF, Kreissig I, Akkoyun I, Kamppeter BA. Intraocular pressure elevation after intravitreal triamcinolone acetonide injection. *Ophthalmology*. 2005;112(4):593-598.
5. Clark AF, Wordinger RJ. The role of steroids in outflow resistance. *Exp Eye Res*. 2009;88(4):752-759.
6. Clark AF, Morrison JC. Steroid-induced glaucoma. In: Morrison JC, Pollack IP, eds. *Glaucoma: Science and Practice*. New York, NY: Thieme; 2003.

Selective Abnormality of Cone Outer Segment Tip Line in Acute Zonal Occult Outer Retinopathy as Observed by Spectral-Domain Optical Coherence Tomography

Optical coherence tomography (OCT) plays an important role in the diagnosis of retinal diseases with minimal ophthalmoscopic changes. For example, in eyes with acute zonal occult outer retinopathy (AZOOR),[1-5] an abnormality of the photoreceptor inner segment–outer segment (IS/OS) junction found by OCT was spatially correlated with the region of visual field defect. Recent high-resolution spectral-domain OCT images have shown a thin line between the IS/OS junction and the retinal pigment epithelium. This line has been identified as the cone OS tip (COST) line.[6] However, the pathophysiological interpretation of its appearance has not been established, and the diagnostic value of the COST line has yet to be determined.

We report 2 cases of AZOOR, both of which showed acute central scotoma with an enlarged blind spot. The ophthalmoscopic and angiographic changes were minimal, but electroretinography (ERG) revealed reduced responses in the affected regions. In both cases, the IS/OS junction on the OCT image was normal, but the COST line was not present or appeared indistinct in the region of visual field defect. Our findings suggest that the COST line may be an early indicator of cone photoreceptor dysfunction in eyes with minimal ophthalmoscopic abnormalities.

Report of Cases. Patient 1 (a 24-year-old woman) and patient 2 (a 28-year-old woman) both had sudden unilateral visual disturbances following photopsia. The visual acuities were 0.02 OD and 1.5 OS in patient 1 and 0.15 OD and 1.5 OS in patient 2. Goldmann kinetic perimetry revealed a blind spot enlargement and central scotoma in the right eye of both patients (**Figure 1** and **Figure 2**). The anterior segment and fundus were normal; however, fluorescein angiography showed a slightly mottled hyperfluorescence around the macula in the affected eye of both patients. The full-field scotopic ERGs were normal, but there were phase delays in the photopic 30-Hz ERGs in the affected eyes: 5.7 milliseconds in patient 1 and 8.0 milliseconds in patient 2. In addition, the amplitudes of the photopic b-waves were reduced in both patients. The focal macular ERGs (ER80; Kowa Co, Tokyo, Japan, and Mayo Co, Nagoya, Japan) in the central 15° were almost flat in the affected eye in both patients. Neither patient had systemic disorders such as viral infections or autoimmune diseases.

Spectral-domain OCT (Carl Zeiss Meditec, Dublin, California) showed the IS/OS junction clearly, even in the region of the scotoma. However, the COST line was not detected in patient 1 and appeared indistinct in patient 2 (Figure 1 andFigure 2). Moreover, the bulgelike structure of the IS/OS junction at the fovea (with the foveal bulge indicating a domelike appearance of the IS/OS junction due to an elongated cone OS at the fovea)[7] could not be observed in the affected eyes. The visual disturbances of these patients did not recover, and these abnormalities in the OCT images were observed at all examinations for 50 months in patient 1 and 18 months in patient 2 after the onset.

Comment. To our knowledge, this is the first report of AZOOR where the boundary of the IS/OS junction in the OCT images was well preserved but the COST line was absent or indistinct from the initial examination through the entire follow-up period. Earlier studies demonstrated that a loss or irregularity of the IS/OS junction observed by OCT corresponded well with the visual field defects even at the early stages of AZOOR,[2-5] and the abnormality in the IS/OS junction can improve following recovery of the scotoma. These findings have led to the hypothesis that photoreceptor OS dysfunction is the primary lesion in AZOOR.

The COST line corresponds to the junction between the photoreceptor tips and the apical processes of the retinal pigment epithelium, where photoreceptor OS disc membranes are continuously shed for renewal.[6] Thus, the appearance of the COST line may reflect the normal function of the photoreceptor OSs more closely than the IS/OS junction. In fact, in all of the AZOOR cases we have recently examined, the COST line was always absent in the region of IS/OS abnormalities, suggesting that the abnormality of the COST line may precede that of the IS/OS junction. In our 2 cases, the fundus appeared normal and the IS/OS junction was clearly observed in the region of the COST line abnormality for 50 and 18 months after the onset. The focal macular ERGs, however, were markedly reduced in the affected areas. In the OCT images, the cone photoreceptor dysfunction corresponding to the region of scotoma could be detected only by the abnormality of the COST line.

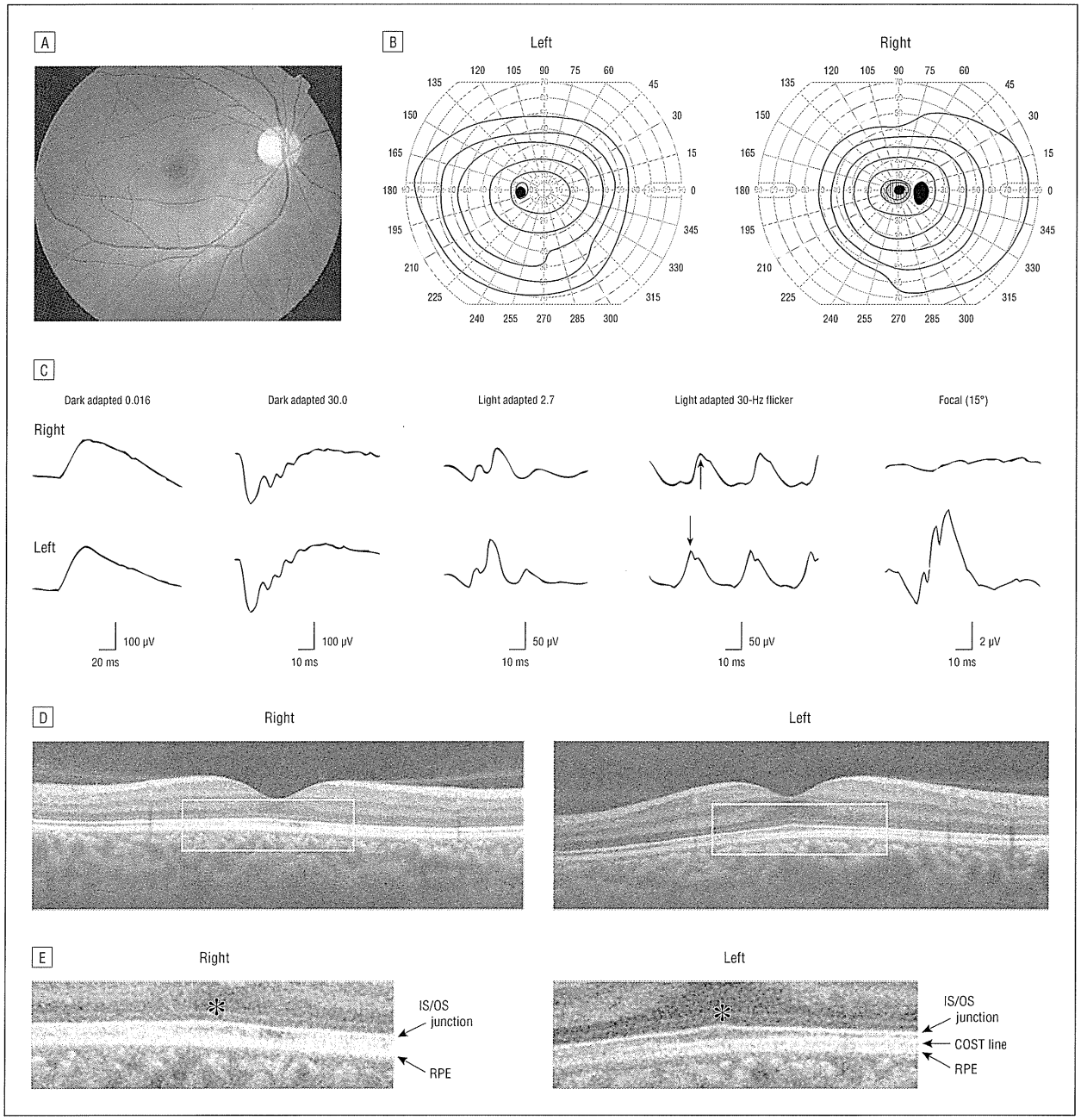

Figure 1. Findings in patient 1. A, Fundus photograph of the right eye showing a normal appearance. B, Goldmann kinetic perimetry showing a blind spot enlargement and central scotoma in the right eye. C, Full-field and focal macular electroretinograms. The latencies of the photopic 30-Hz flicker responses are delayed in the right eye. Arrows indicate the phase difference in light-adapted 30-Hz flicker responses. The focal macular electroretinogram is almost flat in the central 15° of the right eye. Optical coherence tomographic images vertically profiled along the foveola (D) and magnified optical coherence tomographic images in the region of visual field abnormality (E). In the left eye, the inner segment–outer segment (IS/OS) junction, foveal bulge, and cone OS tip (COST) line are clearly observed. In the right eye, the IS/OS junction is clearly observed but the COST line is absent in the macula. The foveal bulge (asterisk) cannot be observed in the right eye. RPE indicates retinal pigment epithelium.

Our findings suggest that the dysfunction of the cone photoreceptor OS could be initially reflected by an absence or indistinctness of the COST line and the absence of the foveal bulge.[5] These changes may be followed by the development of abnormalities in the IS/OS junction in the more advanced stages. However, in our cases, the IS/OS junction remained the same during the entire follow-up period. This may suggest another possibility that our 2 cases constitute a subtype of AZOOR. However, in another case of AZOOR with a blind spot enlargement and relative central scotoma (a 21-year-old woman, data not shown), both the IS/OS and COST lines disappeared in the peripapillary region where visual field disturbance was severe, whereas only the COST line disappeared and the IS/OS line remained normal in the foveal region where the visual field disturbance was milder. These findings support the idea that the visibility of the COST line is more easily affected than that of

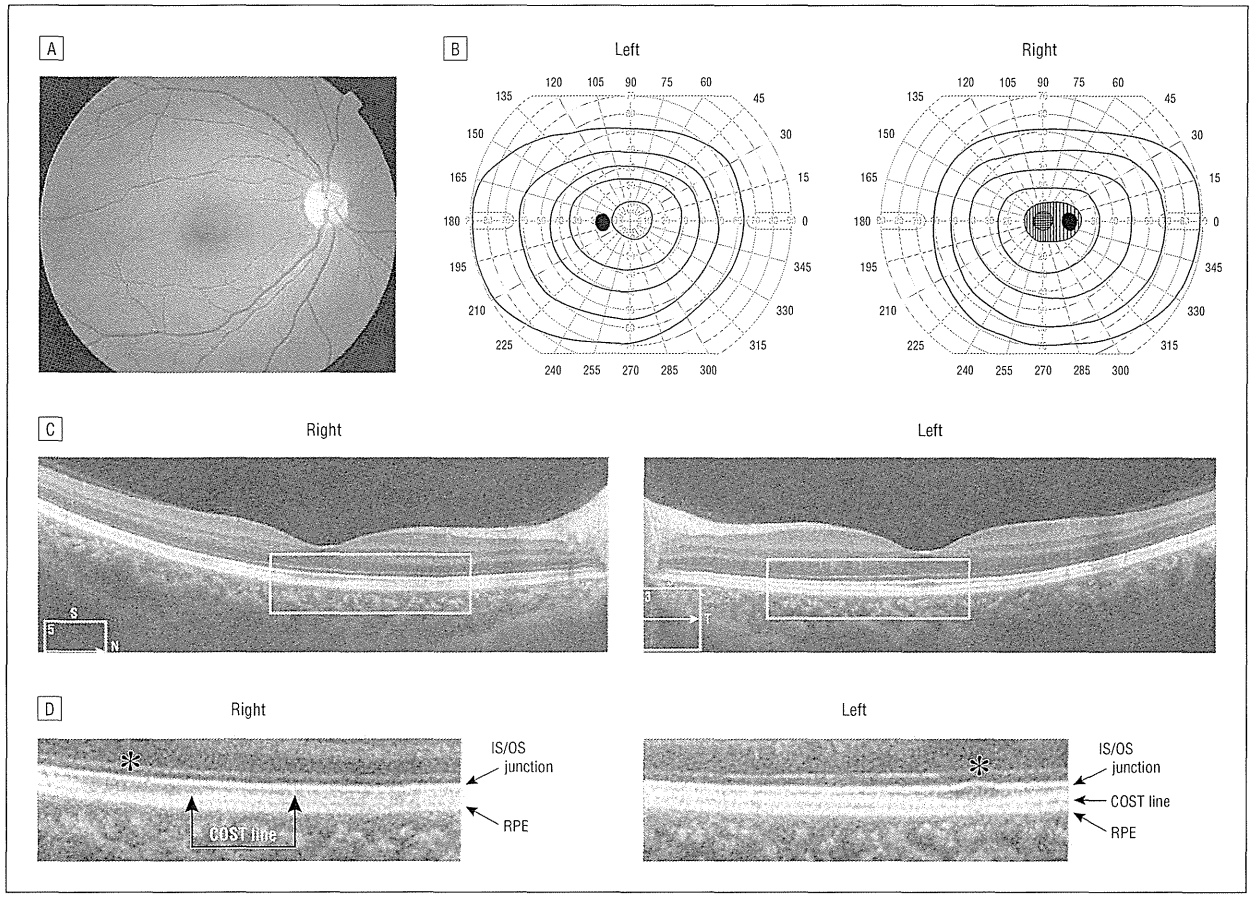

Figure 2. Findings in patient 2. A, Fundus photograph of the right eye showing a normal appearance. B, Goldmann kinetic perimetry showing a blind spot enlargement and central scotoma in the right eye. Optical coherence tomographic images horizontally profiled along the foveola (C), and magnified optical coherence tomographic images in the region of the visual field abnormality (D). In both eyes, the inner segment–outer segment (IS/OS) junction is clearly observed. In the right eye, the cone OS tip (COST) line is partially observed but appeared more indistinct than in the left eye. The foveal bulge (asterisk) cannot be seen in the right eye.

the IS/OS line at an earlier stage by the pathological changes in a typical case of AZOOR. We should note that care should be taken in evaluation of the COST line because its visibility is dependent on the intensity and direction of the laser light that reaches the photoreceptor layer.[6] However, in patients with AZOOR, the COST line and the foveal bulge observed by OCT could help as indicators of early cone photoreceptor dysfunction in cases with minimal ophthalmoscopic and angiographic abnormalities.

Kazushige Tsunoda, MD
Kaoru Fujinami, MD
Yozo Miyake, MD

Author Affiliations: National Institute of Sensory Organs, Tokyo (Drs Tsunoda and Fujinami), and Aichi Medical University, Aichi (Dr Miyake), Japan.
Correspondence: Dr Tsunoda, Laboratory of Visual Physiology, National Institute of Sensory Organs, 2-5-1 Higashigaoka, Meguroku, Tokyo 1528902, Japan (tsunodakazushige@kankakuki.go.jp).
Financial Disclosure: None reported.
Funding/Support: This work was supported by research grants from the Ministry of Health, Labor, and Welfare, Japan, and by SENTAN, Japan Science and Technology Agency, Japan.

1. Gass JD, Agarwal A, Scott IU. Acute zonal occult outer retinopathy: a long-term follow-up study. *Am J Ophthalmol*. 2002;134(3):329-339.
2. Li D, Kishi S. Loss of photoreceptor outer segment in acute zonal occult outer retinopathy. *Arch Ophthalmol*. 2007;125(9):1194-1200.
3. Zibrandtsen N, Munch IC, Klemp K, Jørgensen TM, Sander B, Larsen M. Photoreceptor atrophy in acute zonal occult outer retinopathy. *Acta Ophthalmol*. 2008;86(8):913-916.
4. Spaide RF, Koizumi H, Freund KB. Photoreceptor outer segment abnormalities as a cause of blind spot enlargement in acute zonal occult outer retinopathy-complex diseases. *Am J Ophthalmol*. 2008;146(1):111-120.
5. Takai Y, Ishiko S, Kagokawa H, Fukui K, Takahashi A, Yoshida A. Morphological study of acute zonal occult outer retinopathy (AZOOR) by multiplanar optical coherence tomography. *Acta Ophthalmol*. 2009;87(4):408-418.
6. Srinivasan VJ, Monson BK, Wojtkowski M, et al. Characterization of outer retinal morphology with high-speed, ultrahigh-resolution optical coherence tomography. *Invest Ophthalmol Vis Sci*. 2008;49(4):1571-1579.
7. Curcio CA, Sloan KR, Kalina RE, Hendrickson AE. Human photoreceptor topography. *J Comp Neurol*. 1990;292(4):497-523.

Adult Ovarian Retinoblastoma Genomic Profile Distinct From Prior Childhood Eye Tumor

We report the first case of a woman, previously cured of childhood intraocular retinoblastoma, who developed tumor in the ovary with histological and genomic characteristics suggesting an independent retinoblastoma, not a metastasis.

Transcorneal Electrical Stimulation Promotes Survival of Photoreceptors and Improves Retinal Function in Rhodopsin P347L Transgenic Rabbits

Takeshi Morimoto,[1] *Hiroyuki Kanda,*[1] *Mineo Kondo,*[2] *Hiroko Terasaki,*[3] *Kohji Nishida,*[4] *and Takashi Fujikado*[1]

Purpose. To determine whether transcorneal electrical stimulation (TES) has neuroprotective effects on the photoreceptors, and whether it slows the rate of decrease of the electroretinogram (ERG) in rhodopsin P347L transgenic (Tg) rabbits.

Methods. Six-week-old Tg rabbits received TES through a contact lens electrode on the left eye weekly for 6 weeks. The right eyes received sham stimulation on the same days. Electroretinograms (ERGs) were recorded before and at 12 weeks after the TES. After the last ERG recordings, the animals were euthanized for morphologic analysis of the retinas. Immunohistochemical (IHC) analysis was performed to detect the immunostaining by peanut agglutinin (PNA) and rhodopsin antibodies in the retinas.

Results. The a- and b-wave amplitudes of the photopic ERGs and the b-wave amplitudes of the scotopic ERGs at higher stimulus intensities were significantly larger in the TES eyes than in the sham stimulated eyes ($P < 0.05$, respectively). Morphologic analyses showed that the mean thickness of the outer nuclear layer (ONL) in the visual streak at 12 weeks was significantly thicker in TES eyes than in sham-stimulated eyes ($P < 0.05$). IHC showed that the immunostaining by PNA and rhodopsin antibody in the TES-treated retinas was stronger than that in the sham-stimulated retinas.

Conclusions. TES promotes the survival of photoreceptors and preserves the ERGs in Tg rabbits. Although further investigations are necessary before using TES on patients, these findings indicate that TES should be considered for therapeutic treatment for RP patients with a P347L mutation of rhodopsin. (*Invest Ophthalmol Vis Sci.* 2012;53:4254–4261) DOI: 10.1167/iovs.11-9067

Patients with RP have a progressive loss of rod and cone photoreceptors that leads to a severe decrease in the visual acuity and a severe constriction of the visual field.[1,2] The worldwide prevalence of RP is approximately 1 in 4000, meaning that more than 1 million individuals are affected worldwide.[3] As such, RP is one of the leading causes of blindness in the world.

Many promising treatments to save or restore vision in RP patients are being investigated clinically and experimentally.[4–9] Electrical stimulation (ES) of the retina is one of the methods that is being tried because it is less invasive than other treatments and has been shown to have neuroprotective properties on the visual system.[10–18] ES of the transected optic nerve stump in rats promoted the survival of axotomized retinal ganglion cells (RGCs) in vivo.[10] Transcorneal electrical stimulation (TES) in rats was reported to rescue axotomized RGCs[11,12] and promote axonal regeneration of injured RGCs.[13,14] TES was also shown to improve the visual function of patients with traumatic optic neuropathy and nonarteritic ischemic optic neuropathy.[15]

We have demonstrated that TES promoted the survival of photoreceptors and preserved the retinal function of Royal College of Surgeons (RCS) rats, an animal model of RP.[16] Ni et al.[17] also reported that TES had neuroprotective effects on the photoreceptors after phototoxicity in rats. In a preliminary clinical trial, Schatz et al.[18] demonstrated that TES improved the visual function in RP patients.

However, RP is a genetically heterogeneous disease, and mutations in several photoreceptor-specific and some nonspecific genes are known to cause RP.[19] Therefore, it is necessary to examine the neuroprotective effect of TES on the photoreceptors in the retinas of various RP animal models to determine which genetic type of RP is responsive to TES.

Rhodopsin Pro 347 Leu (P347L) transgenic (Tg) rabbits have been generated by Kondo et al.[20] This sequence of alterations is similar to those in human patients with autosomal dominant RP (adRP) with the rhodopsin P347L mutation.[21,22] This animal model has a rod-dominated, progressive photoreceptor degeneration with regional variations in the pattern of photoreceptor loss.[20,23]

The purpose of this study was to determine whether TES has a neuroprotective effect on the photoreceptors and improves the amplitudes of the electroretinogram (ERG) in Tg rabbits. Our morphologic and electrophysiological analyses showed that TES had a neuroprotective effect on the photoreceptors and improved the amplitudes of the ERG of Tg rabbits.

Materials and Methods

Animals

All experimental procedures were performed in accordance with the ARVO Statement for the Use of Animals in Ophthalmic and Vision

From the [1]Departments of Applied Visual Science and [4]Ophthalmology, Osaka University Graduate School of Medicine, Osaka, Japan; [2]Department of Ophthalmology, Mie University Graduate School of Medicine, Mie, Japan; and [3]Department of Ophthalmology, Nagoya University Graduate School of Medicine, Nagoya, Japan.

Submitted for publication November 12, 2011; revised April 3, 2012; accepted April 25, 2012.

Disclosure: **T. Morimoto**, None; **H. Kanda**, None; **M. Kondo**, None; **H. Terasaki**, None; **K. Nishida**, None; **T. Fujikado**, None

Corresponding author: Takeshi Morimoto, Department of Applied Visual Science, Osaka University Graduate School of Medicine, 2-2 Yamadaoka, Suita City, Osaka 565-0871, Japan; takeshi.morimoto@ophthal.med.osaka-u.ac.jp.

Investigative Ophthalmology & Visual Science, June 2012, Vol. 53, No. 7

Research, and the procedures were approved by the Animal Research Committee, Osaka University Graduate School of Medicine. Five Tg rabbits were purchased from the Kitayama Labes Co. (Ina, Japan). They were raised on a 12-hour dark 12-hour light cycle with an ambient light intensity of 100 lux.

Transcorneal Electrical Stimulation

The rabbits were anesthetized intramuscularly with a mixture of medetomidine (0.3 mg/kg, Domitor; Orion Corporation, Espoo, Finland), midazolam (4 mg/kg, Dormicum, Astellas Pharma Inc., Tokyo, Japan), and butorphanol (5 mg/kg, Betorphal; Meiji Seika Pharma, Co., Ltd., Tokyo, Japan). For the electrical stimulation, the corneas were also anesthetized with a drop of 0.4% oxybuprocaine HCl, and a contact lens electrode with inner and outer concentric electrodes (Mayo Corporation, Nagoya, Japan) was placed on the cornea with a drop of 2.5% methylcellulose to maintain good electrical contact and prevent corneal drying. Biphasic rectangular current pulses (700 μA, 10 ms/phase duration) were delivered at a frequency of 20 Hz from an electrical stimulation system (Stimulator: SEN-7320, Nihon Kohden, Tokyo, Japan; Isolator: WPI, Sarasota, FL) through the contact lens electrode.

TES was given to 6-week-old rabbits for 1 hour once a week until the animals were 12 weeks old. Only the left eye was electrically stimulated. The same type of contact lens electrode was placed on the right eyes but no electrical current was delivered (sham stimulation).

Electroretinograms

ERGs were recorded from the animals at 6 weeks of age just before the beginning of the TES and after the end of the TES treatments at 12 weeks of age. For the TES, animals were anesthetized intramuscularly with a mixture of medetomidine (0.3 mg/kg), midazolam (1 mg/kg), and butorphanol (1 mg/kg). The pupils were dilated with 2.5% phenylephrine hydrochloride and 0.5 % tropicamide.

After 1 hour of dark adaptation, the animals were restrained in a box and were prepared for the recordings under dim red light. ERGs were recorded from both eyes simultaneously with a corneal electrode carrying LEDs creating a mini-Ganzfeld stimulator (WLS-20, Mayo Corporation). A 2.5% hydroxypropyl methylcellulose ophthalmic solution was used with the corneal contact lens electrode. The reference electrode and a ground electrode were inserted subcutaneously into the left ear and the nose, respectively.

The luminance of the scotopic ERG stimuli was increased from −5.0 to 1.48 log cd·s/m^2 in 0.5 or 1.0 log unit steps. After the scotopic ERG recordings, animals were light-adapted for 30 minutes, and the photopic ERGs were recorded. The luminance of photopic ERG stimuli was increased from −1.0 to 1.95 log cd·s/m^2, and the stimuli were presented on a white background of 25 cd/m^2.

The responses were amplified, band pass filtered from 0.3 to 1000 Hz, and digitized at 3.3 kHz. A computational ERG recording system (Neuropack μ; Nihon Kohden, Tokyo, Japan) was used to average the ERG responses. Five to 20 responses were averaged with interstimulus intervals from 1 to 10 seconds depending on the intensity of the stimulus.

ERG Analysis

The scotopic (dark-adapted) and photopic (light-adapted) a-wave amplitudes were measured from the prestimulus baseline to the peak of the a-wave, and the b-wave amplitude was measured from the trough of the a-wave to the peak of b-wave.

To determine the significance of differences in the ERG amplitudes between TES electrically stimulated eyes and sham-stimulated eyes for the full intensity range, we plotted the average ratio of the TES-treated to the sham-stimulated eyes at all intensities and performed statistical analyses.[22–24]

Histological Analysis

Immediately after the final ERG recordings, the rabbits were euthanized with an overdose of pentobarbital sodium. The eyes were removed and placed in a mixture of 10% neutral buffered formalin and 2.5% glutaraldehyde in 0.1 M phosphate buffer (PB) for 30 minutes at room temperature. Then eyes were trimmed, and part of the eye cups, including the optic nerve, were postfixed in 4% glutaraldehyde in 0.1 M PB at 4°C. The tissues were trimmed, embedded in paraffin, sectioned vertically, and stained with hematoxylin and eosin for light microscopy. All sections were cut along the vertical meridian of the eye passing through the optic nerve. Five serial sections of each eye were analyzed for each experimental animal.

The degree of retinal degeneration was assessed by measuring the thickness of the outer nuclear layer (ONL), inner nuclear layer (INL), and ganglion cell layer (GCL). Photographs were taken of the superior and inferior hemispheres at 10 defined points with a camera attached to a light microscope (E800; Nikon, Tokyo, Japan). The first photograph was taken at approximately 2 mm from the center of the optic nerve head, and subsequent photographs were taken every 2 mm more peripherally. The thickness of ONL, INL, and GCL were measured on the photographs (Scion Image analyzer; Scion Corp., Frederick, MD). Each eye was coded so that the investigator making the measurements was masked to treatment of the eye.

Immunohistochemistry

The paraffin-embedded sections (5 μm) were processed for immunofluorescence staining with antirhodopsin antibody (1:100; RET-P1; Santa Cruz Biotechnology, Santa Cruz, CA), followed by Cy3-conjugated anti-mouse IgG (1:200), and FITC-conjugated peanut agglutinin (1:100) (PNA; Invitrogen, Carlsbad, CA), a lectin that binds specifically to rabbit cone photoreceptors. The TES-treated and sham-stimulated sections were observed with a fluorescence microscope (E800; Nikon).

Statistical Analysis

Data were analyzed with a commercial software (JMP8; SAS Institute Japan, Tokyo, Japan). The data were expressed as the means ± SDs or SEMs. Comparisons between two groups were made by Student's *t*-tests when the data were normally distributed or by the Mann-Whitney rank-sum test when the data were not normally distributed. Statistical significance was set at $P < 0.05$.

Results

Effect of TES on Survival of Photoreceptors in Tg Rabbits

Representative retinal sections in the area of the visual streak from 12-week-old Tg rabbits that had TES (left eye) or sham stimulation (right eye) are shown in Figures 1A and 1B. The number of rows of nuclei in the ONL at the visual streak was two to three and the nuclei were closely packed in the retina receiving TES (Fig. 1A). In the sham-stimulated retina, only one row of nuclei was found in the ONL at the visual streak and they were loosely packed (Fig. 1B). In contrast, there was no difference in the structure and thickness of the ONL in other areas of the retina away from the visual streak between the TES-treated and sham-stimulated retinas (Figs. 1C, 1D). The architecture and thickness of the middle and inner retinal layers were well preserved in both TES-treated and sham-stimulated retinas (Figs. 1A–D).

Quantitative analyses showed that the thickness of the ONL in the visual streak in the TES-treated eyes was 13.9 ± 3.3 μm

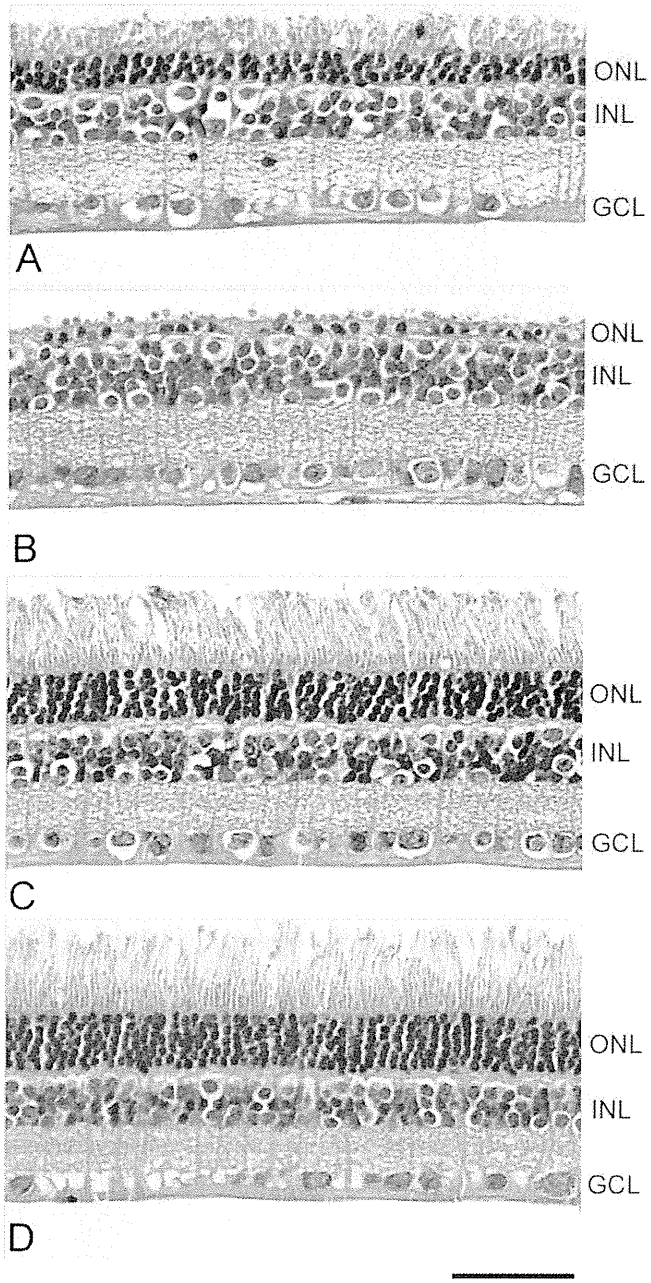

FIGURE 1. Photomicrographs of TES-treated and sham-stimulated retinas from 12-week-old Tg rabbits. Retinal sections of the visual streak from TES-treated retina (**A**) and sham-stimulated retina (**B**). Peripheral retinas at 6 mm superior to the optic nerve head from TES-treated retina (**C**) and sham-stimulated retina (**D**). Scale bar = 50 μm.

(mean ± SD, $n = 5$) which was significantly thicker than that in the sham-stimulated eyes (8.8 ± 2.8 μm, $n = 5$, $P < 0.05$) (inferior hemisphere 1). In contrast, there was no significant difference in the mean ONL thickness outside the area of the visual streak (Fig. 2A). Thus, TES promoted the survival of photoreceptors in the area of the visual streak at 12 weeks of age.

To determine whether TES affected other layers of the retina, we measured the thickness of the INL and GCL. There were no significant differences of the mean thickness of INL and GCL between the TES retinas and in the sham retinas ($n = 5$ each; Figs. 2B, 2C).

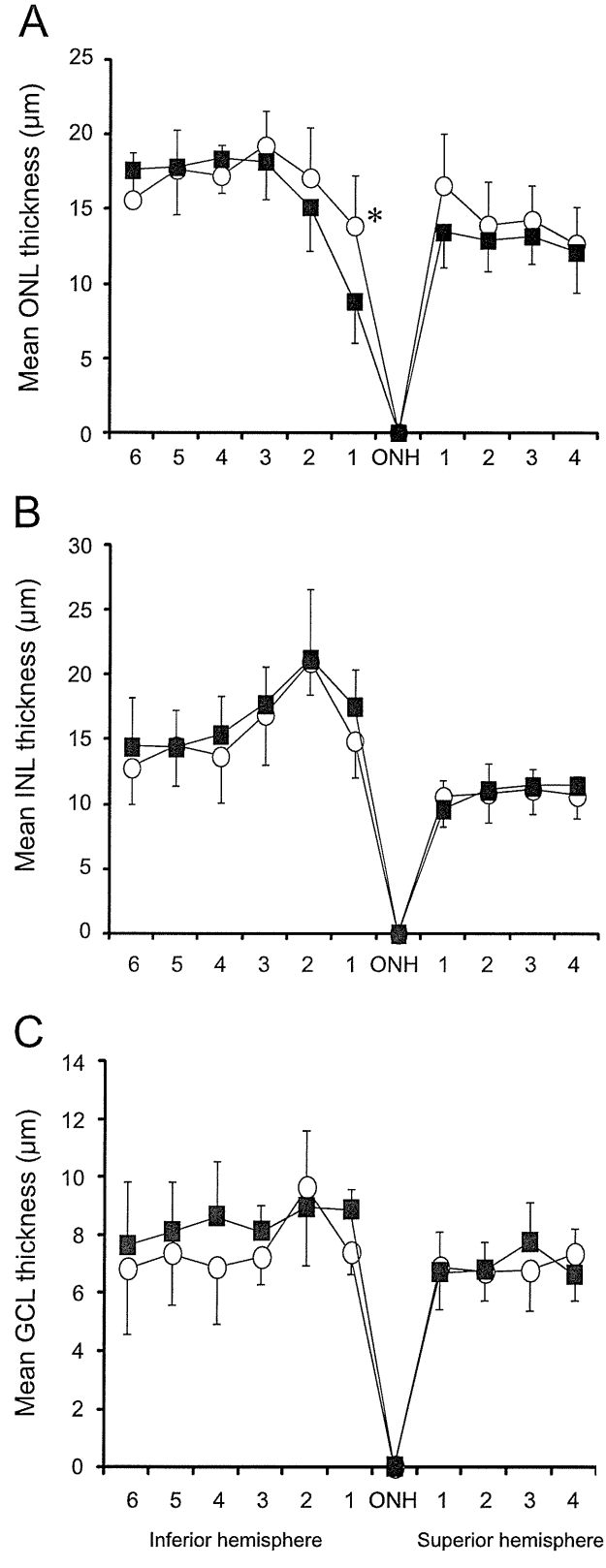

FIGURE 2. Thickness of the ONL (**A**), the INL (**B**), and the GCL (**C**) along the vertical meridian measured at 10 retinal locations at 2-mm intervals. Mean ± SD of five Tg rabbits are plotted. There was a significant difference of the mean ONL thickness between TES-treated retinas (○) and sham-stimulated retina (■) at the visual streak (Student's *t*-test for two groups; $^*P < 0.05$).

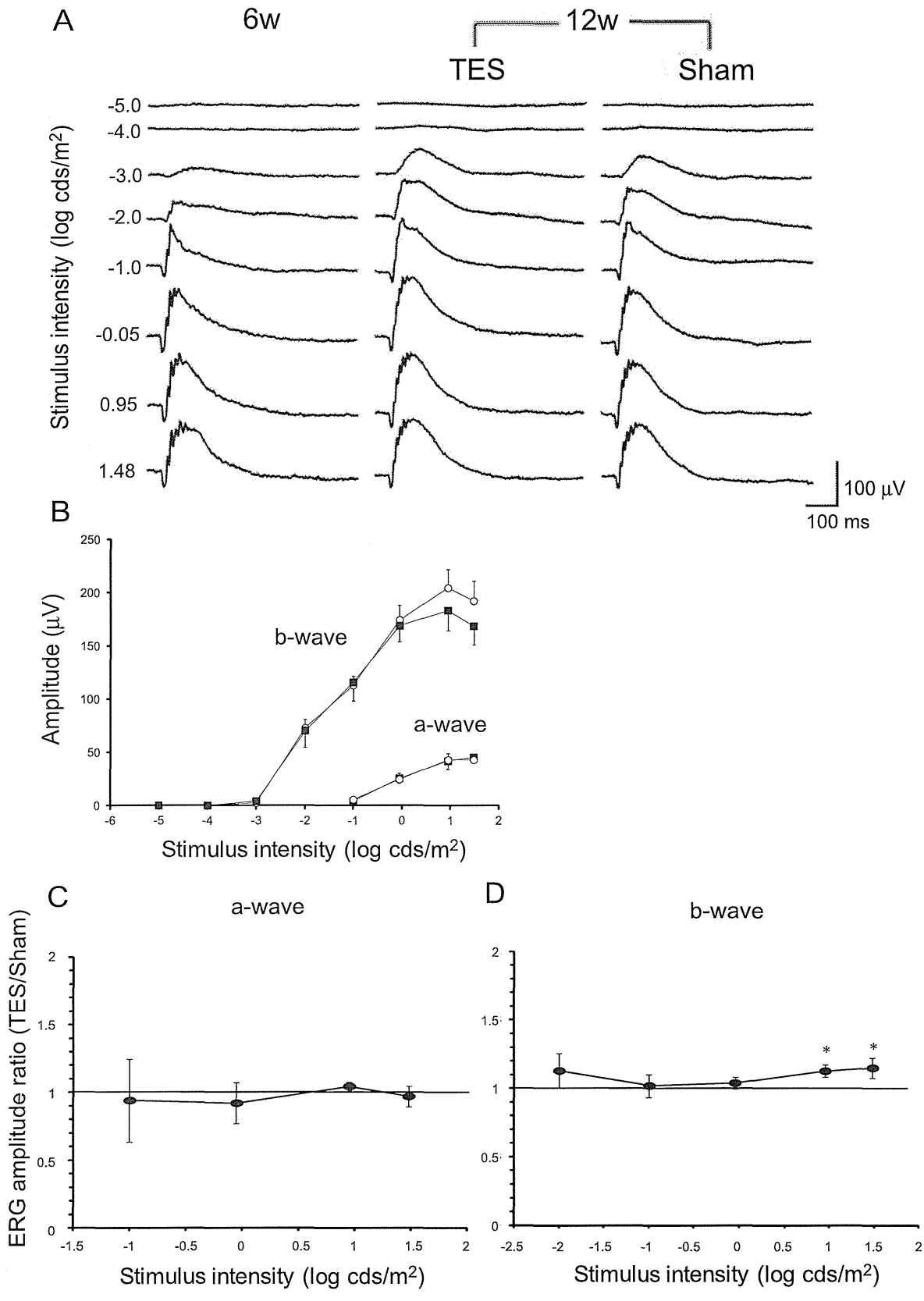

FIGURE 3. Scotopic ERGs recorded from 6- and 12-week-old rhodopsin P347L Tg rabbits. (**A**) Scotopic ERGs elicited by eight different stimulus intensities. (**B**) Scotopic ERG mean amplitude versus flash intensity for the a- and b-waves in the TES-treated (○) and sham-stimulated eyes (■) ($n = 5$, each, mean ± SEM). Average ratio (TES/sham) of the a- (**C**) and b-wave (**D**) amplitudes at 12 weeks of age ($n = 5$, each, mean ± SEM). Pointwise comparison indicated a significant difference in b-wave amplitudes at 1.48 and 0.95 log cd·s/m^2 (Student's *t*-tests for two groups; $^*P < 0.05$).

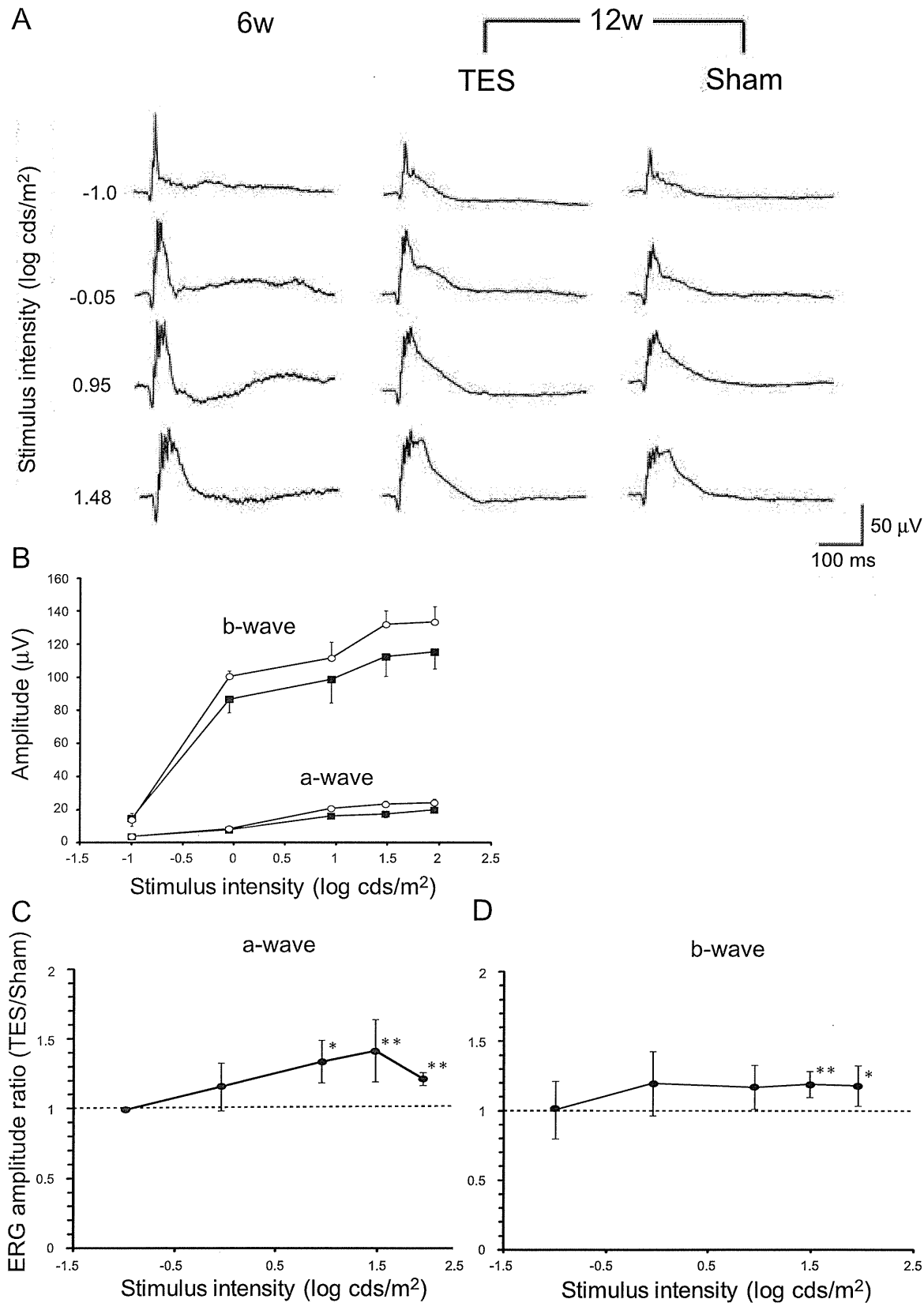

FIGURE 4. Photopic ERGs recorded from 6- and 12-week-old rhodopsin P347L Tg rabbits. (**A**) Photopic ERGs elicited by five different stimulus intensities. (**B**) Photopic ERG mean amplitude versus flash intensity for the a- and b-waves in the TES-treated (○) and sham-stimulated (■) retinas. Average ratio (TES/sham) of the a- (**C**) and b-wave (**D**) amplitudes at 12 weeks of age ($n = 5$, each, mean ± SEM). Pointwise comparison indicated a significant difference in a-wave amplitudes at 0.95 to 1.95 log cd·s/m^2 (Student's *t*-tests for two groups; $^*P < 0.05$, $^{**}P < 0.01$), and in b-wave amplitudes at 1.48 and 1.95 log cd·s/m^2 (Student's *t*-tests for two groups; $^*P < 0.05$, $^{**}P < 0.01$).

Effect of TES on Electroretinograms of Tg Rabbits

To evaluate the electrical properties of the rod and cone systems of rabbits, we recorded full-field scotopic and photopic ERGs. The scotopic ERGs elicited by different stimulus intensities from 6- and 12-week-old Tg rabbits are shown in Figure 3A. The amplitudes of the scotopic ERGs recorded from the eyes of 12-week-old Tg rabbits were not reduced compared with those from the eyes of 6-week-old Tg rabbits. The intensity–response curves for the a- and b-waves are plotted in Figure 3B. Scotopic ERG a-wave amplitudes of TES-treated eyes were not significantly different from those of sham-stimulated eyes. However, the b-wave amplitudes of the TES-treated eyes were slightly but significantly larger than those of the sham-stimulated eyes at the higher stimulus intensities.

We plotted the ratio (TES/sham-stimulated eye) of the amplitudes of the a- and b-waves for all intensities and performed statistical analyses on the differences (Figs. 3C, 3D). The differences in the ratios of the a-waves were not significant for all intensities. On the other hand, the ratios of the b-wave amplitudes were significantly larger at stimulus intensities higher than 0.95 log cd·s/m^2 ($P < 0.05$) in the TES-treated eyes.

The photopic ERGs obtained from Tg rabbits at 6 and 12 weeks of age are also shown in Figure 4A. The amplitudes of the TES-treated and sham-stimulated eyes at 12 weeks of age were slightly reduced compared with the ERGs recorded from 6-week-old Tg rabbits but the differences were not significant. However, the responses in the eye treated with TES were larger than those treated with sham stimulation (Fig. 4A).

The intensity–response curve for the a- and b-waves are plotted in Figure 4B. We also plotted the average ratio of TES-treated to sham-stimulated eyes at all intensities (Figs. 4C, 4D). For a-waves, there were significant differences between TES-treated and sham-stimulated eyes at 0.95 to 1.95 log cd·s/m^2 ($P < 0.05$, respectively). For b-waves, there were significant differences between them at 1.48 and 1.95 log cds/m^2 ($P < 0.05$).

Immunohistochemistry

Immunostaining with an antirhodopsin antibody and PNA lectin showed that the intensities of the immunostaining for both antirhodopsin antibody and PNA were stronger in the TES-treated retina (Figs. 5A–C) than the sham-stimulated retina (Figs. 5D–F).

Discussion

Our electrophysiological and histological analyses showed that TES led to the survival of photoreceptors in the visual streak, and it also led to the preservation of ERG responses at higher stimulus intensities in rhodopsin P347L Tg rabbits. Although the cause of the photoreceptor degeneration in Tg rabbits is different from that in RCS rats and the phototoxic-induced degeneration in rats,[20,23,25–27] TES also had a neuroprotective effect on the photoreceptors in Tg rabbits. These findings indicate that TES might have a similar neuroprotective effect on photoreceptors whose degeneration has different causes.

In the histological analysis, only the photoreceptors in the visual streak were rescued by TES, and in the areas outside the visual streak, the number of photoreceptors in the TES-treated retina was not significantly different from that in sham-stimulated retina. In Tg rabbits, the loss of photoreceptors was maximum in the visual streak where the photoreceptor density is highest, and the loss of photoreceptors was not significantly different at other regions outside visual streak at 12 weeks of age.[20] Therefore, at 12 weeks of age, the loss of photoreceptors was striking only in the visual streak, indicating that the neuroprotection of photoreceptors was limited to the visual streak.

Immunohistochemical analysis showed that the intensity of both PNA and rhodopsin immunostainings was stronger in the TES-treated retinas than in the sham-stimulated retinas in the visual streak.

However, the results of ERGs indicated that TES preserved the cone components better than rod components, although in Tg rabbits the rod components are more affected than the cones.[20,23] Although it was not determined why the cone components were better preserved than the rod components, one possibility is that TES promoted the survival of both rod and cone photoreceptors, and the rescued rods secreted a cone viability factor to rescue the cone photoreceptors.[28] Otherwise, at 12 weeks of age, photoreceptors near the visual streak were much more affected than those outside the visual streak,[20] therefore the differences of ERG amplitudes of full field ERGs between TES-treated and sham-stimulated retinas might be detected only at higher stimulus intensities.

There are some possible mechanisms for the neuroprotection of photoreceptors. First, TES increased the expression of the mRNA and protein levels of neurotrophic factors (e.g., insulin-like growth factor-1 (IGF-1), brain-derived neurotrophic

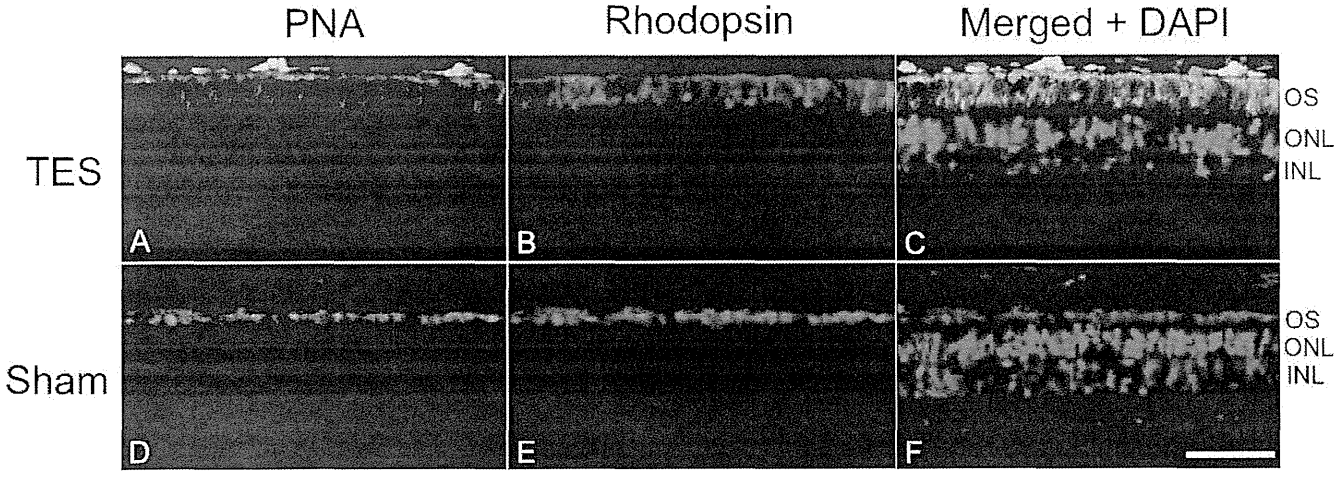

Figure 5. Immunohistochemical analysis of rod and cone photoreceptors triple labeled with rhodopsin (*green*), PNA (*red*), and DAPI (*blue*) in TES-treated (**A–C**) and sham-stimulated retinas (**D–E**) at 12 weeks of age (approximately 4 mm inferior to the optic nerve head). Intensities of rhodopsin and PNA immunostaining are stronger in the TES-treated ratio than in the sham-stimulated retina. Scale bar = 50 μm.

factor (BDNF), ciliary neurotrophic factor, or B-cell lymphoma-2 in the retinas after TES.[11,17] A second possibility is that TES reduced the expression of the TNF super families and Bax, which are related to apoptosis signaling in retinal cells.[29] Cultured rat Müller cells exposed to electrical currents have been shown to express IGF-1, BDNF, and fibroblast growth factor-2 (FGF-2).[30–32] Other types of electrical stimulation to the retinas, such as subretinal electrical stimulation, increases the expression of FGF-2 in the retinas.[33] Unfortunately, we did not determine whether the expression of any of these neurotrophic factors was increased after TES in the Tg rabbit retinas.

Another possible mechanism for the TES-induced neuroprotection was an increase of chorioretinal blood circulation by TES.[34,35] In clinical studies, TES has been shown to improve the visual function of patients with retinal artery occulsion.[36,37] Thinning of the vascular plexus and the development of aberrant vessels have been reported in RP patients and animal models of RP.[38–41] This indicates that retinal blood circulation might be reduced in Tg rabbits. TES might have some neuroprotective effects on photoreceptors by increasing chorioretinal blood circulation.

We did not examine whether TES was neuroprotective for the photoreceptors in the peripheral retina. In Tg rabbits at the age of 48 weeks, almost all of the photoreceptors were lost[20,27]; however, it takes a long time to investigate the neuroprotective effects of TES on the entire retina until the age of 48 weeks from 6 weeks, so it is difficult to continue the treatment until 48 weeks because weekly anesthesia and treatment put a heavy load on animals and is adverse to the animal welfare for long-term experiments. The results that TES did have neuroprotective effects on photoreceptors in the visual streak at 12 weeks of age were enough to lead us to determine the neuroprotection of TES on the photoreceptors in Tg rabbits.

Rhodopsin P347L Tg rabbits are an adRP model of human RP. Our results indicate that TES might have a neuroprotective effect on the photoreceptors in RP patients with the same mutation. Schatz et al.[18] performed a prospective, randomized sham-controlled clinical study, and reported that TES improved the visual function in RP patients. From these neuroprotective effects of TES already published and our results, TES might exert a neuroprotective effect on photoreceptors of different animals with RP. Additional investigations on different animal models are necessary to determine which type of RP was the indication of TES treatment.

In conclusion, TES had a neuroprotective effect on the photoreceptors in the visual streak of rhodopsin P347L Tg rabbits, which is a model of human adRP. These results support and encourage clinical trials of TES for RP patients.

Acknowledgments

The authors thank Yuko Furukawa and Emi Higasa for technical assistance, and Duco I. Hamasaki for help with the manuscript.

References

1. Marmor MF, Aguirre G, Arden G, et al. Retinitis pigmentosa: a symposium on terminology and methods of examination. *Ophthalmology.* 1983;90:126–131.
2. Pagon RA. Retinitis pigmentosa. *Surv Ophthalmol.* 1988;33:137–177.
3. Hartong DT, Berson EL, Dryja TP. Retinitis pigmentosa. *Lancet.* 2006;368:1795–1809.
4. Berson EL, Rosner B, Sandberg MA, et al. A randomized trial of vitamin A and vitamin E supplementation for retinitis pigmentosa. *Arch Ophthalmol.* 1993;111:761–772.
5. Sieving PA, Caruso RC, Tao W, et al. Ciliary neurotrophic factor (CNTF) for human retinal degeneration: phase I trial of CNTF delivered by encapsulated cell intraocular implants. *Proc Natl Acad Sci U S A.* 2006;103:3896–3901.
6. Ali RR, Sarra GM, Stephens C, et al. Restoration of photoreceptor ultrastructure and function in retinal degeneration slow mice by gene therapy. *Nat Genet.* 2000;25:306–310.
7. Bainbridge JW, Smith AJ, Barker SS, et al. Effect of gene therapy on visual function in Leber's congenital amaurosis. *N Engl J Med.* 2008;358:2231–2239.
8. Zrenner E, Bartz-Schmidt KU, Benav H, et al. Subretinal electronic chips allow blind patients to read letters and combine them to words. *Proc Biol Sci.* 2011;278:1489–1497.
9. Fujikado T, Kamei M, Sakaguchi H, et al. Testing of semichronically implanted retinal prosthesis by suprachoroidal-transretinal stimulation in patients with retinitis pigmentosa. *Invest Ophthalmol Vis Sci.* 2011;52:4726–4733.
10. Morimoto T, Miyoshi T, Fujikado T, Tano Y, Fukuda Y. Electrical stimulation enhances the survival of axotomized retinal ganglion cells in vivo. *NeuroReport.* 2002;13:227–230.
11. Morimoto T, Miyoshi T, Matsuda S, Tano Y, Fujikado T, Fukuda Y. Transcorneal electrical stimulation rescues axotomized retinal ganglion cells by activating endogenous retinal IGF-1 system. *Invest Ophthalmol Vis Sci.* 2005;46:2147–2155.
12. Morimoto T, Miyoshi T, Sawai H, Fujikado T. Optimal parameters of transcorneal electrical stimulation (TES) to be neuroprotective of axotomized RGCs in adult rats. *Exp Eye Res.* 2010;90:285–291.
13. Miyake K, Yoshida M, Inoue Y, Hata Y. Neuroprotective effect of transcorneal electrical stimulation on the acute phase of optic nerve injury. *Invest Ophthalmol Vis Sci.* 2007;48:2356–2361.
14. Tagami Y, Kurimoto T, Miyoshi T, Morimoto T, Sawai H, Mimura O. Axonal regeneration induced by repetitive electrical stimulation of crushed optic nerve in adult rats. *Jpn J Ophthalmol.* 2009;53:257–266.
15. Fujikado T, Morimoto T, Matsushita K, Shimojo H, Okawa Y, Tano Y. Effect of transcorneal electrical stimulation in patients with nonarteritic ischemic optic neuropathy or traumatic optic neuropathy. *Jpn J Ophthalmol.* 2006;50:266–273.
16. Morimoto T, Fujikado T, Choi JS, et al. Transcorneal electrical stimulation promotes the survival of photoreceptors and preserves retinal function in royal college of surgeons rats. *Invest Ophthalmol Vis Sci.* 2007;48:4725–4732.
17. Ni YQ, Gan DK, Xu HD, Xu GZ, Da CD. Neuroprotective effect of transcorneal electrical stimulation on light-induced photoreceptor degeneration. *Exp Neurol.* 2009;219:439–452.
18. Schatz A, Röck T, Naycheva L, et al. Transcorneal electrical stimulation for patients with retinitis pigmentosa: a prospective, randomized, sham-controlled exploratory study. *Invest Ophthalmol Vis Sci.* 2011;23:4485–4496.
19. Daiger SP, Bowne SJ, Sullivan LS. Perspective on genes and mutations causing retinitis pigmentosa. *Arch Ophthalmol.* 2007;125:151–158.
20. Kondo M, Sakai T, Komeima K, et al. Generation of a transgenic rabbit model of retinal degeneration. *Invest Ophthalmol Vis Sci.* 2009;50:1371–1377.
21. Oh KT, Longmuir R, Oh DM, et al. Comparison of the clinical expression of retinitis pigmentosa associated with rhodopsin mutations at codon 347 and codon 23. *Am J Ophthalmol.* 2003;136:306–313.
22. Berson EL, Rosner B, Sandberg MA, et al. Ocular findings in patients with autosomal dominant retinitis pigmentosa and rhodopsin, proline-347-leucine. *Am J Ophthalmol.* 1991;111:614–623.
23. Sakai T, Kondo M, Ueno S, et al. Supernormal ERG oscillatory potentials in transgenic rabbit with rhodopsin P347L mutation

and retinal degeneration. *Invest Ophthalmol Vis Sci.* 2009;50: 4402–4409.

24. Bush RA, Lei B, Tao W, et al. Encapsulated cell-based intraocular delivery of ciliary neurotrophic factor in normal rabbit: dose-dependent effects on ERG and retinal histology. *Invest Ophthalmol Vis Sci.* 2004;45:2420–2430.
25. D'Cruz PM, Yasumura D, Weir J, et al. Mutation of the receptor tyrosine kinase gene Mertk in the retinal dystrophic RCS rat. *Hum Mol Genet.* 2000;9:645–651.
26. Noell WK, Walker VS, Kang BS, Berman S. Retinal damage by light in rats. *Invest Ophthalmol.* 1966;5:450–473.
27. Jones BW, Kondo M, Terasaki H, et al. Retinal remodeling in the Tg P347L rabbit, a large-eye model of retinal degeneration. *J Comp Neurol.* 2011;519:2713–2733.
28. Léveillard T, Mohand-Saïd S, Lorentz O, et al. Identification and characterization of rod-derived cone viability factor. *Nat Genet.* 2004;36:755–759.
29. Willmann G, Schäferhoff K, Fischer MD, et al. Gene expression profiling of the retina after transcorneal electrical stimulation in wildtype brown Norway rats. *Invest Ophthalmol Vis Sci.* 2011;52:7529–7537.
30. Sato T, Lee TS, Takamatsu F, Fujikado T. Induction of fibroblast growth factor-2 by electrical stimulation in cultured retinal Mueller cells. *Neuroreport.* 2008;19:1617–1621.
31. Sato T, Fujikado T, Morimoto T, Matsushita K, Harada T, Tano Y. Effect of electrical stimulation on IGF-1 transcription by L-type calcium channels in cultured retinal Müller cells. *Jpn J Ophthalmol.* 2008;52:217–223.
32. Sato T, Fujikado T, Lee TS, Tano Y. Direct effect of electrical stimulation on induction of brain-derived neurotrophic factor from cultured retinal Müller cells. *Invest Ophthalmol Vis Sci.* 2008;49:4641–4646.
33. Ciavatta VT, Kim M, Wong P, et al. Retinal expression of Fgf2 in RCS rats with subretinal microphotodiode array. *Invest Ophthalmol Vis Sci.* 2009;50:4523–4530.
34. Kurimoto T, Oono S, Oku H, et al. Transcorneal electrical stimulation increases chorioretinal blood flow in normal human subjects. *Clin Ophthalmol.* 2010;4:1441–1446.
35. Mihashi T, Okawa Y, Miyoshi T, Kitaguchi Y, Hirohara Y, Fujikado T. Comparing retinal reflectance changes elicited by transcorneal electrical retinal stimulation with those of optic chiasma stimulation in cats. *Jpn J Ophthalmol.* 2011;55:49–56.
36. Inomata K, Shinoda K, Ohde H, et al. Transcorneal electrical stimulation of retina to treat longstanding retinal artery occlusion. *Graefes Arch Clin Exp Ophthalmol.* 2007;245: 1773–1780.
37. Oono S, Kurimoto T, Kashimoto R, Tagami Y, Okamoto N, Mimura O. Transcorneal electrical stimulation improves visual function in eyes with branch retinal artery occlusion. *Clin Ophthalmol.* 2011;5:397–402.
38. Spalton DJ, Bird AC, Cleary PE. Retinitis pigmentosa and retinal oedema. *Br J Ophthalmol.* 1978;62:174–182.
39. Uliss AE, Gregor ZJ, Bird AC. Retinitis pigmentosa and retinal neovascularization. *Ophthalmology.* 1986;93:1599–1602.
40. Matthes MT, Bok D. Blood vascular abnormalities in the degenerative mouse retina (C57BL/6J-rd le). *Invest Ophthalmol Vis Sci.* 1984;25:364–369.
41. Wang S, Villegas-Pérez MP, Vidal-Sanz M, Lund RD. Progressive optic axon dystrophy and vacuslar changes in rd mice. *Invest Ophthalmol Vis Sci.* 2000;41:537–545.

Ophthalmic Genetics, 33(2), 83–88, 2012

ISSN: 1381-6810 print/1744-5094 online
DOI: 10.3109/13816810.2011.634877

informa
healthcare

RESEARCH REPORT

Clinical features of a Japanese case with Bothnia dystrophy

Kazutoshi Nojima[1], Katsuhiro Hosono[1], Yang Zhao[1,2], Takaaki Toshiba[1], Akiko Hikoya[1], Tatsuhiko Asai[1], Masaru Kato[3], Mineo Kondo[4], Shinsei Minoshima[2], and Yoshihiro Hotta[1]

[1]*Department of Ophthalmology, Hamamatsu University School of Medicine, Hamamatsu, Japan,* [2]*Department of Photomedical Genomics, Basic Medical Photonics Laboratory, Medical Photonics Research Center, Hamamatsu University School of Medicine, Hamamatsu, Japan,* [3]*Department of Ophthalmology, Seirei Mikatahara Hospital, Hamamatsu, Japan, and* [4]*Department of Ophthalmology, Nagoya University Graduate School of Medicine, Nagoya, Japan*

ABSTRACT

Purpose: Bothnia dystrophy is a variant of recessive retinitis punctata albescens (RPA) and is caused by a homozygous R234W mutation in the *RLBP1* gene. We report the clinical features of a Japanese patient with the homozygous R234W mutation in the *RLBP1* gene.

Methods: An affected woman with RPA has been examined clinically for 25 years. Her DNA was obtained with informed consent, and the exons and surrounding areas of *RDH5*, rhodopsin, and *RLBP1* were amplified by PCR and directly sequenced.

Results: Our patient was first examined in our hospital in 1986 when she was 6 years old. Ophthalmoscopy showed numerous small white dots in the posterior pole of both eyes. Although the a- and b-waves of the single flash ERGs were severely reduced after a standard 30 min of dark-adaptation, the amplitudes of both waves increased markedly after 24 hr of dark-adaptation. The visual disturbances and visual field scotomas became more evident in her twenties, and her BCVAs were 0.2 OD and 0.5 OS when she was 31 years old in 2010. Fundus examinations showed macular degeneration in both eyes. A homozygous R234W mutation was detected in *RLBP1*, and no mutations were detected in *RDH5* and rhodopsin.

Conclusions: The clinical characteristics of a Japanese patient with a homozygous R234W mutation in *RLBP1* are very similar to that of Swedish patients with Bothnia dystrophy. The origin of the Japanese R234W mutation is probably not the same as that of the Swedish patients, but more likely due to the high incidence of C to T transitions.

Keywords: Retinitis punctata albescens, Bothnia dystrophy, *RLBP1* gene, *RDH5* gene, electroretinograms

INTRODUCTION

The flecked retina syndrome includes benign (familial) flecked retina, fundus albipunctatus, and retinitis punctata albescens (RPA) (OMIM #136880, 228980). The benign (familial) flecked retina is typically not associated with nyctalopia or a delay in dark-adaptation.[1] Although young patients with fundus albipunctatus and RPA can have similar symptoms and signs, RPA is progressive and associated with a severe decrease in the amplitudes of the electroretinograms (ERGs). The amplitudes do not recover even after prolonged dark-adaptation. The retinal changes can progress to generalized atrophy of retina.

Mutations in the *RDH5* gene have been found in patients with fundus albipunctatus in various ethnic groups and also in patients with cone dystrophy associated with fundus albipunctatus.[2–5] A consanguineous Saudi Arabian kindred with a retinal dystrophy phenotype that fulfilled the criteria of fundus albipunctatus in younger individuals and RPA in older patients with the R150Q mutation of *RLBP1* gene has also been reported.[6] Mutations in the genes encoding rhodopsin (*RHO*), peripherin/RDS (*PRPH2*),

Received 19 June 2011; revised 19 September 2011; accepted 01 October 2011

Correspondence: Yoshihiro Hotta, MD, Department of Ophthalmology, Hamamatsu University School of Medicine, 1-20-1 Handayama, Hamamatsu 431–3192, Japan. Tel: +81 53 435 2256. Fax: +81 53 435 2372. E-mail: hotta@hama-med.ac.jp

and retinaldehyde-binding protein (*RLBP1*) have been reported in patients with RPA,[7–12] whereas *RLBP1* gene mutations cause autosomal recessive retinitis pigmentosa, RPA, fundus albipunctatus, and Newfoundland rod-cone dystrophy (OMIM# 607476).[9,13,14]

Bothnia dystrophy (BD, OMIM#607475) is an atypical form of RPA and is caused by an arginine-to-tryptophan missense mutation at position 234, R234W, in the *RLBP1* gene.[15] We report a Japanese case of RPA with a homozygous R234W mutation suggesting a Japanese case of BD. We were able to follow our patient for 25 years and confirmed the significant recovery of the full-field ERGs after 24 hrs of dark-adaptation.

MATERIALS AND METHODS

Patient

A 6-year-old Japanese girl was first examined in our hospital in 1986 because of night blindness which was first noticed at the age of 2 years. She underwent periodic ophthalmological examinations over the next 25 years in the Department of Ophthalmology, Hamamatsu University Hospital, Hamamatsu, Japan. None of the individuals in her family had BD or other ocular diseases. Her father and mother are not relatives but her paternal ancestors were from Shinshiro city and her maternal ancestors from Mikawaichinomiya-cho. These cities are in the Aichi prefecture and are situated close to each other.

The visual acuity (VA) was determined using a decimal visual acuity chart. The visual fields were determined with a Goldmann perimeter using standard targets. The course of dark-adaptation was determined with a Goldmann-Weekers adaptometer. Color vision was tested with the Ishihara pseudoisochromatic plates (38 plates; 2002 edition) and Panel D-15 test.

Electroretinographic Analyses

Full-field ERGs were elicited with a Ganzfeld dome and recorded with a unipolar contact lens electrode. The reference and ground electrodes were attached to the forehead and the ipsilateral ear, respectively. After 30 min of dark-adaptation, a rod response was elicited by a white flash at an intensity of 0.01cd-s/m^{-2}. Single-flash cone responses and 30 Hz flicker responses were elicited by white stimuli of 3.0cd-s/m^{-2} on a white background of 81cd/m^{-2}. Maximal rod-cone responses were elicited by a bright white flash (20 Joules) at an intensity of 10.0cd-s/m^{-2}. The maximal rod-cone responses were also recorded after a prolonged dark-adaptation of 3 hrs and 24 hrs when the patient was 7 and 32 years old.

Mutation Analyses

This study was approved by the Institutional Review Board for Human Genetic and Genome Research of the Hamamatsu University School of Medicine, and procedures were performed in accordance with the Declaration of Helsinki. An informed consent was obtained from the patient. Genomic DNA was extracted from peripheral lymphocytes by standard procedures. Polymerase chain reaction (PCR) was performed using the KOD -Plus-ver.2 (TOYOBO, Japan) with published primers[16] and the primer sets shown in Table 1. PCR was performed according to the manufacturer's protocol at

TABLE 1 PCR primer sequences for *RDH5*, *RHO*, and *RLBP1*

		PCR primer		
Gene	Exon	Forward	Reverse	PCR product size (bp)
*RDH5**	2	GGCCACAGTAAACTGGACAA	TTCCTGGTGGTCTACCATAC	405
	3	CCCCAGCATCCTTTTCATCT	GGTCACAAAGCTTACATAAGGGTA	454
	4	AAGAACCCAGCAACTTCGCT	TTCCCTTCATGTGCCCCTGT	237
	5	CTGATTGCAACCACCTATGG	CAATCTCTTGCTGGAAGGCT	276
RHO	1	AATATGATTATGAACACCCCCAAT	ACCTAGGACCATGAAGAGGTCAG	460
	1	ACTTCCTCACGCTCTACGTCAC	GCACAAACAGCAGCCCGGCTAT	385
	2	TCCTTCCCCAAGGCCTCCTCAA	GGTCAGTGCCTGGAACCAGACA	402
	3	AGCCATGCAGACGTTTATGAT	CTTCTGTGTGGTGGCTGACT	454
	4	GTCTTCACCGTCAAGGAGGTA	CTGACCCAAGACTGCTGCCAGT	498
	5	CTCAAGCCTCTTGCCTTCCAGT	GGTGGATGTCCCTTCTCAGGCTG	331
RLBP1	3	GCCTCGGGTGATTCTGATGCAAT	ACCCACACAGGGGTTATAGAAG	334
	4	CAGGCTGATGCGGTTGGCTGTT	AGTCTATCAGGTCCAGGATGATCT	302
	5	GCTCTGGCAGGAGACTCATCAC	CCCACAGTATGGAAGCAGGCCT	393
	6	ACTAGGAGGGATGGGGTAGGGAT	GAACCAGGAATGAGGGCCCAGT	331
	7	TCCGAGATCAAAGCCTGCAGCAA	AATACTTGGCAAACTGTCAATCAC	467
	8	GTGATGCTGGACAAGTCTGTTCTA	TAGCTCAGGACCATGGTAGAGTGT	315
	9	ACTGACACCCAACATGGAGAC	CAGCCCTTTCCTAGCCTTGGGT	394

**RDH5* primers have been previously described.[16]